



1 Spatial and temporal dynamics of suspended sediment concentrations in coastal waters of South  
2 China Sea, off Sarawak, Borneo: Ocean colour remote sensing observations and analysis

3 Jenny Choo<sup>1</sup>, Nagur Cherukuru<sup>2</sup>, Eric Lehmann<sup>2</sup>, Matt Paget<sup>2</sup>, Aazani Mujahid<sup>3</sup>, Patrick Martin<sup>4</sup>, Moritz Müller<sup>1</sup>

4 <sup>1</sup>Swinburne University of Technology, Faculty of Engineering, Computing and Science, Jalan Simpang Tiga, 93350 Kuching,  
5 Sarawak, Malaysia.

6 <sup>2</sup>Commonwealth Scientific and Industrial Research Organization (CSIRO), Canberra ACT 2601, Australia.

7 <sup>3</sup>Faculty of Resource Science & Technology, University Malaysia Sarawak, Kota Samarahan 94300, Sarawak, Malaysia.

8 <sup>4</sup>Asian School of the Environment, Nanyang Technological University, 639798, Singapore.

9  
10 Correspondence to: Jenny Choo (JChoo@swinburne.edu.my/jccy89@gmail.com)

## 12 Abstract

13 High-quality ocean colour observations are increasingly accessible to support various monitoring and  
14 research activities for water quality measurements. In this paper, we present a newly developed  
15 regional total suspended solids (TSS) empirical model using MODIS-Aqua's Rrs(530) and Rrs(666)  
16 reflectance bands to investigate the spatial and temporal variation of TSS dynamics along the  
17 southwest coast of Sarawak, Borneo. The performance of this TSS retrieval model was evaluated using  
18 error metrics (bias = 1.0, MAE = 1.47, and RMSE = 0.22 in mg/L) with a log<sub>10</sub> transformation prior to  
19 calculation, as well as a k-fold cross validation technique. The temporally averaged map of TSS  
20 distribution, using daily MODIS-Aqua satellite datasets from 2003 until 2019, revealed large TSS  
21 plumes detected particularly in the Lupar and Rajang coastal areas on a yearly basis. The average TSS  
22 concentration range of 15 – 20 mg/L was estimated at these coastal areas. Moreover, the spatial map  
23 of TSS coefficient of variation (CV) indicated strong TSS variability (approximately 90 %) in the  
24 Samunsam-Sematan coastal areas, which could potentially impact nearby coral reef habitats in this  
25 region. **Our findings** on temporal TSS variation provide further evidence that monsoonal patterns drive  
26 the TSS release in these tropical water systems, with distinct and widespread TSS plume variations  
27 observed between the northeast and southwest monsoon periods. Map of relative TSS distribution  
28 anomalies revealed strong spatial TSS variations in the Samunsam-Sematan coastal areas, while 2010  
29 recorded a major increase (approximately 100 %) and widespread TSS distribution with respect to the  
30 long-term mean. Furthermore, **our findings** on the contribution of river discharge to the TSS  
31 distribution showed a weak correlation across time at both the Lupar and Rajang river mouth points.  
32 The variability of TSS distribution across coastal river points was studied by investigating the variation  
33 of TSS pixels at three transect points, stretching from the river mouth into territorial and open water  
34 zones, for eight main rivers. **Our findings** showed a progressively decreasing pattern of nearly 50 % in  
35 relation to the distance from shore, with exceptions in the northeast regions of the study area.  
36 Essentially, our findings demonstrate that the TSS levels at the southwest coast of Sarawak are within  
37 local water quality standards, promoting various marine and socio-economic activities. This study  
38 presents the first observation of TSS distributions at Sarawak coastal systems with the application of  
39 remote sensing technologies, to enhance coastal sediment management strategies for the sustainable  
40 use of coastal waters and their resources.

In abstract, our findings  
is not suitable use in writing abstract

41 Keywords: total suspended solids, band-ratio, monsoon, river discharge, Open Data Cube

42

43

44



45 1.0 Introduction

46 Total Suspended Solids (TSS) play an important role in the aquatic ecosystem as one of the primary  
47 water quality indicators of coastal and riverine systems (Alcântara et al., 2016; Cao et al., 2018; Chen  
48 et al., 2015a; González Vilas et al., 2011; Mao et al., 2012). For example, elevated concentrations of  
49 TSS in water have an adverse impact on fisheries and biodiversity of the aquatic ecosystem (Bilotta  
50 and Brazier, 2008; Chapman et al., 2017; Henley et al., 2000; Wilber and Clarke, 2001). Understanding  
51 the impacts of varying water quality in relation to TSS status has been one of the primary concerns  
52 with respect to a country's growing Blue Economy status and sustainable management of aquatic  
53 resources (Lee et al., 2020a; Sandifer et al., 2021; World Bank and United Nations Department of  
54 Economic and Social Affairs (UNDESA), 2017). With about 40 % of the world's population living within  
55 100 km of coastal areas (United Nations, 2017), and with more than 80 % of the population in Malaysia  
56 living within 50 km of the coast (Praveena et al., 2012), water quality monitoring and management  
57 efforts are important at both regional and global scale.

58 Studying TSS distribution can provide insights into the connections between land and ocean  
59 ecosystems (Howarth, 2008; Lemley et al., 2019; Lu et al., 2018). For instance, TSS dynamics allow us  
60 to understand the impacts of sediment transport and sediment plumes, particularly in areas  
61 experiencing large-scale deforestation, land conversion and damming of rivers (Chen et al., 2007;  
62 Espinoza Villar et al., 2013). Sarawak, Malaysian Borneo, experienced significant land use and land  
63 cover change activities over the past four decades, with widespread land conversion and deforestation  
64 for developments and large-scale plantation activities (Gaveau et al., 2016), as well as building of  
65 major road infrastructures, such as the Pan-Borneo highway, and hydroelectric dams (Alamgir et al.,  
66 2020). As a result, river and coastal systems may potentially drive large TSS loads into downstream  
67 systems and into the marine and open ocean waters.

68 Situated at the southern part of the South China Sea, the region of Sarawak, Malaysian  
69 Borneo, has a coastline of about 1035 km where mangrove forests are dominant (Long, 2014). The



70 coastal regions of Sarawak are rich with marine coastal biodiversity and coral reefs, which can be  
71 found at the northeast and southwest part of Sarawak (Praveena et al., 2012). While the coasts of  
72 Sarawak provide important socio-economic values to the local communities (Lee et al., 2020b), these  
73 coastal areas are potentially facing water quality degradation from TSS riverine outputs in response  
74 to land use and land cover change activities.

75 TSS concentrations are commonly measured through conventional laboratory-based methods  
76 to quantify TSS concentrations by field collection of water samples (Ling et al., 2016; Mohammad Razi  
77 et al., 2021; Soo et al., 2017; Soum et al., 2021; Tromboni et al., 2021; Zhang et al., 2013). Currently,  
78 real-time high-frequency TSS observations using modern optical and bio-sensor systems are also  
79 possible (Bhardwaj et al., 2015; Horsburgh et al., 2010). These sensors can be generally found onboard  
80 ship and buoy-based observation platforms. Yet, it remains a challenge to quantify TSS concentrations  
81 of large spatial coverage and high temporal frequency with these approaches.

82 Ocean colour remote sensing technologies represent an increasingly accessible and powerful  
83 tool to provide a synoptic view for short or long-term water quality studies at high temporal and spatial  
84 resolutions (Cherukuru et al., 2016a; Slonecker et al., 2016; Swain and Sahoo, 2017; Wang et al., 2017;  
85 Werdell et al., 2018). Remote sensing can help overcome several constraints of conventional intensive  
86 field campaigns such as: (i) costly field campaigns from boat rentals or cruise; (ii) time-consuming and  
87 inadequate manpower; and most importantly for this study, (iii) limited spatial and temporal field  
88 coverage. NASA's Moderate Resolution Imaging Spectroradiometer (MODIS)-Aqua  
89 (<https://modis.gsfc.nasa.gov/about/>) has a distinctive advantage with its daily revisit time, a spatial  
90 resolution of 250 – 1000 m, and a large collection of ocean colour data since 2002. Other sensors  
91 offering ocean colour measurement capabilities include Landsat-8, which, in comparison with MODIS-  
92 Aqua, has a 16-day revisit time and high spatial resolution of 30 m. Despite Landsat's powerful ability  
93 in capturing higher resolution images, the longer revisit interval may not be suitable for characterizing  
94 and studying water bodies with high dynamics of various water constituents.



95           Several MODIS-derived models have been developed for TSS retrievals (Chen et al., 2015b;  
96 Espinoza Villar et al., 2013; Jiang and Liu, 2011; Kim et al., 2017; Zhang et al., 2010b), including  
97 empirical, semi-analytical and machine-learning approaches (Balasubramanian et al., 2020; Jiang et  
98 al., 2021). However, the performance of these models proved to be less satisfactory, with recorded  
99 low  $r^2$  and high bias and mean absolute error (MAE) values when tested with in situ TSS datasets  
100 (Supplementary Materials, Table S1). While these global TSS remote sensing models address the need  
101 to improve TSS retrievals and to monitor global TSS trends in various water class types, they tend to  
102 underperform in more localised and regional studies (Mao et al., 2012; Ondrusek et al., 2012). The  
103 coastal waters of Borneo are well-mixed throughout the year and enriched with suspended material  
104 and dissolved organic matter (Müller et al., 2016). Various water quality studies of the river systems  
105 have been actively carried out to assess the dynamics of numerous water quality constituents in  
106 response to human activities, with TSS concentrations being one of the primary environmental  
107 concerns in this region (Ling et al., 2016; Müller-dum et al., 2019; Tawan et al., 2020). Although studies  
108 on the water quality of coastal systems in Borneo have gradually gained much attention (Cherukuru  
109 et al., 2021; Limcih et al., 2010; Martin et al., 2018; Soo et al., 2017), there is still much knowledge to  
110 gain on the understanding of how coastal waters in the region have been impacted by TSS loadings  
111 and transport over large spatial and temporal scales.

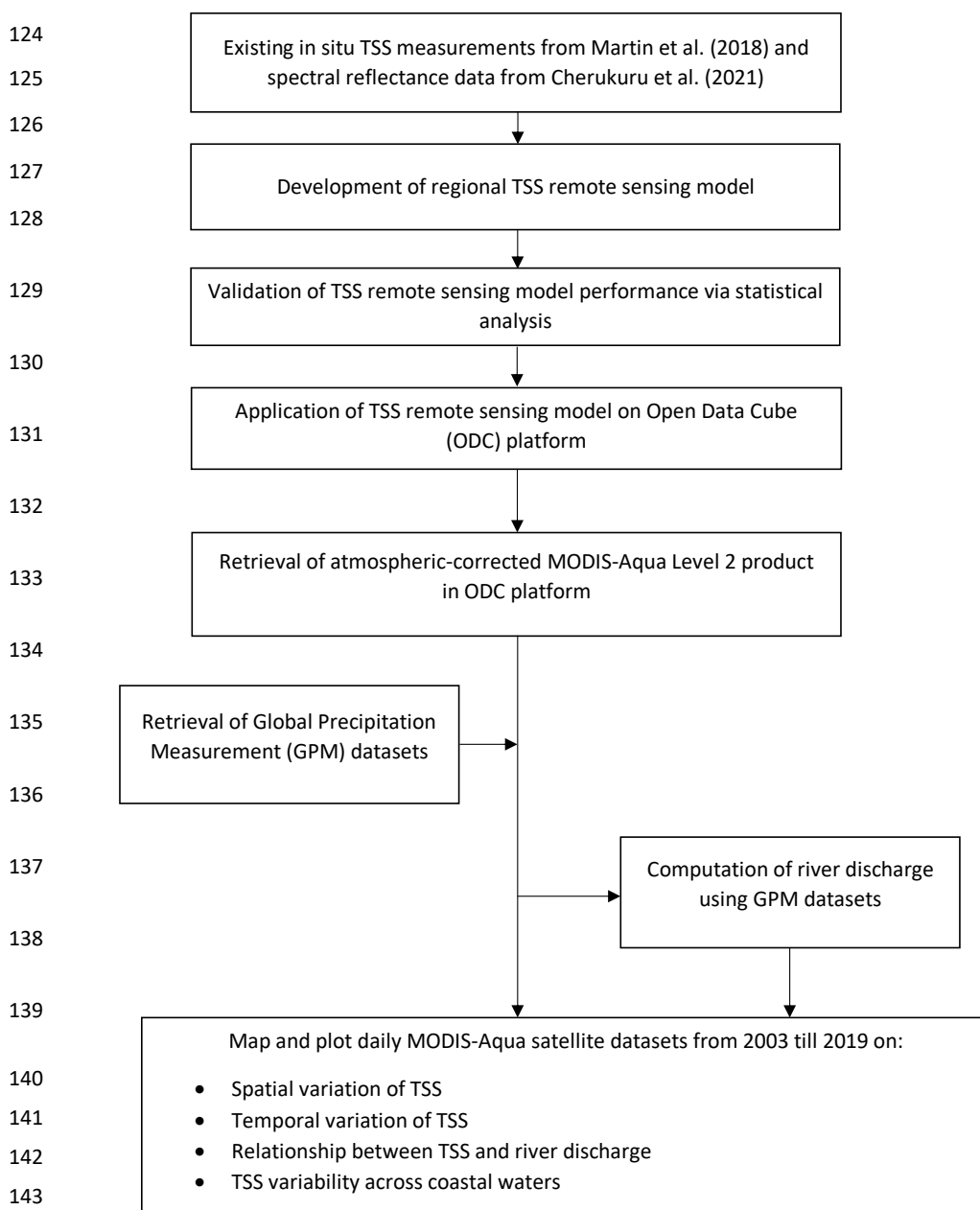
112           Here, in this paper, we present a new regional empirical TSS remote sensing model. While  
113 various remote sensing models have their own unique computational strengths, this **paper**  
114 demonstrates the reliability of band ratio TSS model to be applied within optically complex waters.  
115 With the ongoing efforts to address and minimize water quality degradation in coastal systems, as  
116 outlined in the United Nation's Sustainability Development Goals no. 14, our study aims to apply the  
117 new empirical regional TSS remote sensing model to: (a) investigate the spatial and temporal  
118 variability in TSS, (b) identify hotspots of TSS distribution in the coastal waters of Sarawak, Malaysian  
119 Borneo, using a long time series of MODIS-Aqua data from year 2003 until 2019, and (c) study the  
120 varying monsoonal and river discharge patterns in relation to TSS distribution at river mouths.

Suggested to change to this study



121 2.0 Methodologies

122 Figure below summarizes the processes carried out in this study. Spatial and temporal variation of TSS  
123 distribution was mapped using atmospheric-corrected MODIS-Aqua Level 2 product.





144 Fig. 1: Flowchart summarizing the processes of developing a regional TSS remote sensing model and applying it to analyse  
145 the spatial and temporal variation of TSS over the study region, using MODIS-Aqua data from year 2003 until 2019. Long-  
146 term MODIS-Aqua datasets were analysed and mapped on an Open Data Cube (ODC) platform with implementation of robust  
147 Python libraries and packages.

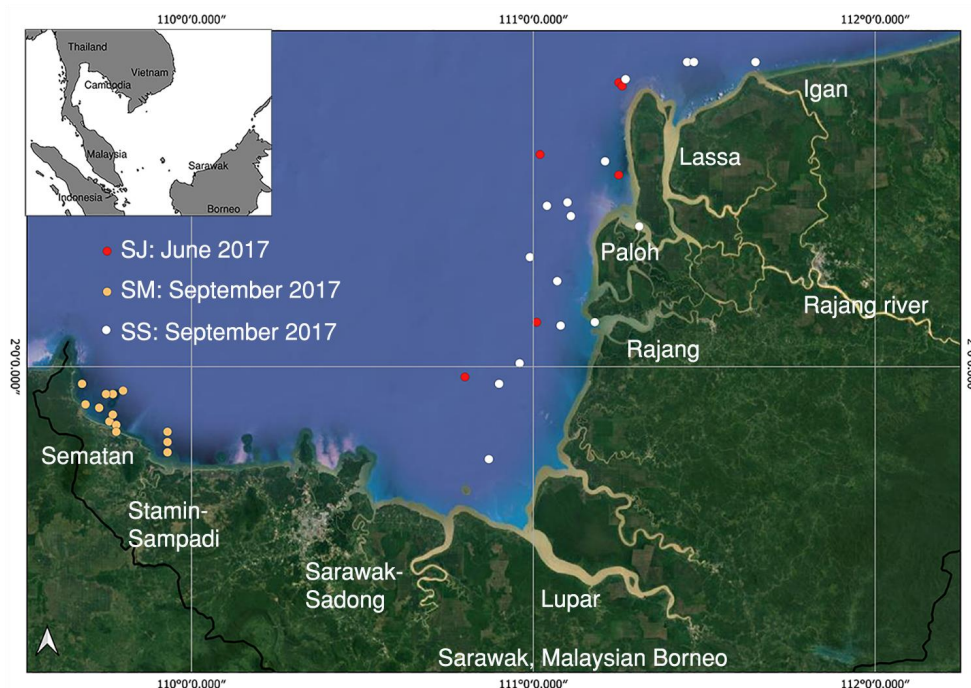
148

## 149 2.1 Area of study

150 Our study focuses on the southwestern coast of Sarawak (between 1.9° N, 109.65° E and 2.8° N, 111.5°  
151 E) in Malaysia, which sits at the northwest part of the Borneo Island. Generally, the island of Borneo  
152 (between 3.01° S, 112.18° E and 6.45° N, 117.04° E) contains rich tropical rainforests and biodiversity  
153 on the lands of Sarawak and Sabah (Malaysia), Brunei, and Indonesia. Typically, Sarawak is a tropical  
154 climate region, recording an average ambient temperature of 27.8 °C (variation of 1.8 °C) throughout  
155 the year. It records high precipitation with an average of 4116.7 mm/yr in Kuching (1.5535° N,  
156 110.3593° E), the capital city of Sarawak. Yearly, it experiences both a dry and wet season, which is  
157 influenced by: (i) the southwestern monsoon (May to September) and (ii) the northeastern monsoon  
158 (November to March). Rivers in Sarawak are connected to the South China Sea and flow through  
159 various plantation types, such as oil palm, rubber and sago (Davies et al., 2010).

160 In this study, **we** studied the southwestern part of Sarawak's coastal regions (Fig. 2), (between 1.9° N,  
161 109.65° E and 2.8° N, 111.5° E), which comprise several major rivers (e.g. Lupar, Sebuyau, Sematan),  
162 as well as the Rajang River, the longest river in Malaysia. These river systems are associated with  
163 increasing land use activities and land cover changes in this region, which essentially transport and  
164 connect various biogeochemical water components to the coastal systems of Sarawak.

Avoid the use of first person pronouns in the manuscript



165

166 Fig. 2: Map of the study area (© Google Maps), located in the southwestern part of Sarawak, Malaysia (inset). Indicators  
167 show the location of sampling sites used during field expeditions carried out in June and September 2017.

### 168 2.2 In situ TSS measurements

169 TSS measurements data were taken from Martin et al. (2018). A total of 35 coastal sites were studied  
170 and are denoted SJ, SS, and SM (see: Table 1 & Fig. 2). These water samples were collected in the  
171 month of June (SJ region) and September (SS and SM regions) in 2017. Water samples were filtered,  
172 and filters were dried and ashed prior to weighing process. Full details of water sampling and TSS  
173 analysis is available in Martin et al. (2018).

### 174 2.3 Development, calibration and validation of TSS model

175 In situ remote sensing reflectance spectral data,  $R_{rs}(\lambda)$ , along with 35 measured TSS values, were used  
176 to develop a new remote sensing TSS empirical model for MODIS-Aqua for this case study. Field



177 measurements of SM, SJ & SS datasets, as shown in Table 1, were used to calibrate the MODIS-Aqua  
178 TSS remote sensing model.

179 For the in situ remote sensing reflectance,  $R_{rs}(\lambda)$  readings, a TriOS-RAMSES spectral imaging  
180 radiometer was used to measure downwelling irradiance,  $E_d(\lambda)$ , and upwelling radiance,  $L_u(\lambda)$ , with  
181 measurement protocols from Mueller et al. (2002). These measurements were recorded under stable  
182 sky and sea conditions during the day (10AM to 4PM) with high-sun elevation angle condition.

183 Measurements of reflectance,  $R_{rs}(\lambda)$ , were recorded concurrently with the collection of water samples  
184 (as described in Section 2.2) and were recorded at wavelength ranging from 280 to 950 nm, which  
185 covers the spectrum of ultraviolet, visible and visible/ultraviolet light. These measurements were  
186 recorded on a float to capture  $L_u(0-, \lambda)$  and  $E_d(0+, \lambda)$ , where 0- and 0+ refer to below-surface and  
187 above-surface, respectively.

188 Remote sensing reflectance,  $R_{rs}(\lambda)$ , was computed as follows with reference to Mueller et al. (2002):

$$R_{rs}(\lambda, 0+) = \frac{1 - p}{n^2} \times \frac{L_u(0-, \lambda)}{E_d(0+, \lambda)} \quad (1)$$

189 where  $p = 0.021$  refers to the Fresnel reflectance and  $n = 1.34$  is the refractive index of water. Full  
190 details of this methodology can be found at Cherukuru et al. (2021).

### 191 2.3.1 Calibration of empirical model and application to MODIS-Aqua

192 With the intention to apply regional TSS remote sensing model to MODIS-Aqua product, a total  
193 number of 35 TSS datasets were collected in coastal conditions (salinity > 15 PSU) and convolved to  
194 generate MODIS-Aqua data.

195 In this study, retrieval of water constituents was established using spectral band ratio combinations  
196 which have proven to be a straightforward, yet reliable method for estimating water constituents in  
197 optically turbid waters (Ahn and Shanmugam, 2007; Cao et al., 2018; Lavigne et al., 2021; Morel and  
198 Gentili, 2009; Neil et al., 2019; Siswanto et al., 2011). Band ratio models help to offset signal noise,



199 such as the effects of atmospheric and irradiance of spectral reflectance to a certain degree  
 200 (Cherukuru et al., 2016b; Ha et al., 2017; Hu et al., 2012; Liu et al., 2019).

201 A variety of models using single bands, as well as a combination of MODIS-Aqua’s Blue, Green & Red  
 202 bands (412nm, 440nm, 488nm, 532nm, 555nm & 660nm) were calibrated using field measurements  
 203 as dependent variable. The calibration process was tested out using various model functions, including  
 204 linear, power, exponential, and logarithm functions. The best empirical TSS retrieval model was fitted  
 205 by means of a regression between the in situ TSS data and in situ radiometer values, and can be  
 206 expressed as follows:

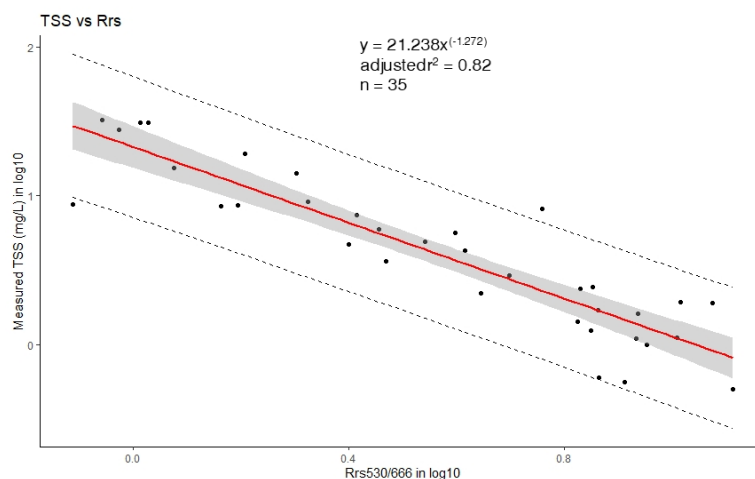
$$207 \quad \text{TSS} = 21.238[\text{Rrs}(530)/\text{Rrs}(666)]^{-1.272} \quad (2)$$

208 This power function model resulted in a coefficient of determination ( $R^2$ ) of 0.82 (Fig. 3).

209 Table 1: Summary statistics of TSS values collected at areas SJ, SS, and SM located within coastal regions in this study, with a  
 210 total of 35 datasets recorded.

Coastal Area	Minimum	Maximum	Mean	S.D.	C.V.	n
SJ	1.1	19.24	6.89	6.62	96.09	6
SS	0.56	32.1	12.50	11.43	91.45	16
SM	0.5	8.14	2.59	2.70	104.53	13

211



212



213 Fig. 3: Empirical relationship of TSS retrieval between in situ Rrs(530)/Rrs(666) bands ratio and measured TSS  
 214 concentration (mg/L), as established via a power law function. Upper and lower dashed lines indicate the 95 % prediction  
 215 interval of the regression.

### 216 2.3.2 Performance assessment and validation of MODIS-Aqua empirical model

217 An evaluation of the model was performed using a k-fold cross validation technique (Refaeilzadeh et  
 218 al., 2020) given the small size of the TSS dataset used in this study (Table 2). A selection of k = 7 was  
 219 assigned to split the datasets into k groups with an equal number of data points.

220 An assessment of the performance error of the newly developed TSS model was carried out as per  
 221 Seegers et al. (2018)'s recommendation for interpreting ocean colour models. These performance  
 222 metrics used here include the bias, Mean Absolute Error (MAE), Root Mean Squared Error (RMSE),  
 223 coefficient of variation (CV), as well as the coefficient determination,  $r^2$ , based on the following  
 224 calculations:

$$225 \text{ Bias} = 10^{\wedge} \left[ \frac{\sum_{i=1}^n \log_{10}(Mi) - \log_{10}(Oi)}{n} \right] \quad (3)$$

$$226 \text{ MAE} = 10^{\wedge} \left[ \frac{\sum_{i=0}^n | \log_{10}(Mi) - \log_{10}(Oi) |}{n} \right] \quad (4)$$

$$227 \text{ RMSE} = \sqrt{\frac{\sum_{i=1}^n (\log_{10}(Mi) - \log_{10}(Oi))^2}{n}} \quad (5)$$

$$228 \text{ CV} = \frac{\sigma}{\mu} \times 100\% \quad (6)$$

229 where M represents the modelled TSS values, n is the number of samples, and O represents the  
 230 observed TSS measurements, while  $\sigma$  refers to standard deviation and  $\mu$  represents the mean value.

231 Equation (3), (4) and (5) use a log<sub>10</sub>-transform of the data as the range of TSS values can span several  
 232 orders of magnitude. As such, an application of the log-transform prior to error metric calculation  
 233 allows us to account for uncertainties that are proportional to the concentration values  
 234 (Balasubramanian et al., 2020; Seegers et al., 2018).

235 Table 2: Assessment of fitting error for the proposed TSS model, using k-fold cross validation.

Parameter	k-fold (n)	R2	RMSE	MAE
TSS	7	0.85	0.2159	0.1747

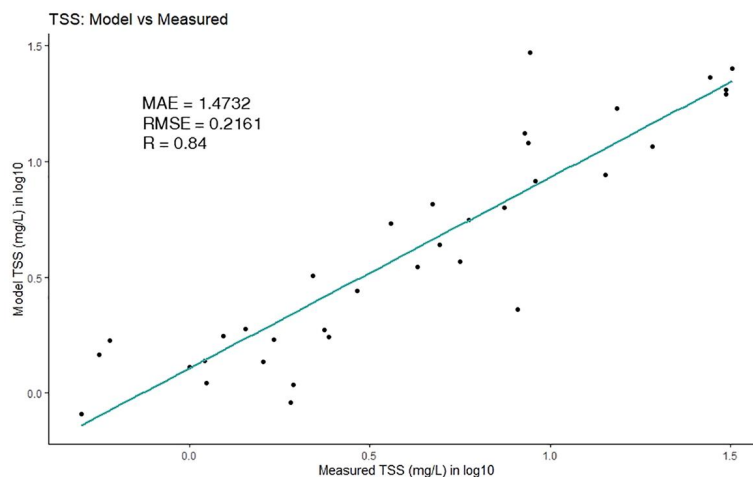


236

237 Table 3: Calibration and accuracy assessment of the newly derived MODIS-Aqua models in this study for TSS estimations.  
 238 Calculation for bias, MAE and RMSE use a log-transform of the data prior to calculation of error metric measurements, as  
 239 adapted from Seegers et al. (2018) and Balasubramanian et al. (2020).

Parameter	Bands (nm)	Model	Bias	MAE	RMSE	CV (%)	R
TSS	Rrs(530), Rrs(666)	TSS = $21.238[(Rrs530/Rrs666)]^{-1.272}$	0.9999	1.4732	0.2161	4.74	0.84

240



241

242 Fig. 4: Scatterplot of modelled TSS values derived from the proposed model and measured TSS values (mg/L). Check  
 243 decimals in figure

244 While these results point to low error levels achieved by the proposed regional TSS retrieval model  
 245 (Table 3, Fig. 4), caution should be used when applying it to various water types. Water type  
 246 classification has been thoroughly described by Balasubramanian et al. (2020) where waters are  
 247 classed into Type I (Blue-Green waters), Type II (Green waters), and Type III (Brown waters).  
 248 Essentially, the Green-to-Red band ratio is optimised with these datasets corresponding to sediment-  
 249 dominated and yellow-substance loaded water conditions. As highlighted by Morel & Belanger (2006),  
 250 this type of waters is not spectrally consistent to phytoplankton-rich waters (also known as Case 1  
 251 waters). In addition to the impact on water clarity, sediment particles (often red-brownish coloured)  
 252 also tend to enhance the backscattering and absorption properties, especially at shorter wavelengths  
 253 (Babin et al., 2003), while the additional presence of coloured dissolved matter (yellow substance)



254 leads to strong absorption properties at short wavelengths. As the TSS retrieval model was developed  
255 from samples taken in waters that are bio-optically rich in suspended solids and dissolved organic  
256 matter, an application of this TSS model needs to be done cautiously when applying to other water  
257 types, particularly those with large concentration of phytoplankton.

#### 258 2.4 Application of TSS retrieval model

259 Daily MODIS-Aqua satellite data from year 2003 to 2019 (total of 6192 individual time slices) were  
260 studied with a 2°x 2° spatial resolution (longitude: 109.38, 112.0; latitude: 1.22, 3.35) which covers  
261 the southwestern coastal region of Sarawak and southern part of the South China Sea.  
262 Atmospherically corrected MODIS-Aqua level 2 reflectance products (Bailey et al., 2010; NASA Official,  
263 n.d.) were retrieved for the application of the TSS model proposed in this study. Negative remote  
264 sensing reflectance values, possibly due to failure of atmospheric correction, were filtered out before  
265 applying the retrieval model, as expressed in Eq. (2), to map the spatial and temporal distribution of  
266 TSS estimates. In addition, averaging of spatial and temporal TSS variation maps in this study was  
267 carried out by filtering TSS values with fewer than 10 valid data points over the whole time series,  
268 along with application of sigma clipping operation Check format of writing  
269 ([https://docs.astropy.org/en/stable/api/astropy.stats.sigma\\_clip.html](https://docs.astropy.org/en/stable/api/astropy.stats.sigma_clip.html))

##### 270 2.4.1 Open Data Cube

271 In this study, the analysis of remote sensing data over large spatial extents and at high temporal  
272 resolution was carried out using robust Python libraries and packages run on an Open Data Cube (ODC)  
273 platform. Open Data Cube is an open-source advancement in computing technologies and data  
274 architectures which addresses the growing volume of freely available Earth Observation (EO) satellite  
275 products (Giuliani et al., 2020; Killough, 2019). ODC provides a collection of software which index,  
276 manage, and process large EO datasets such as satellite products from the MODIS, Landsat and  
277 Sentinel missions (Gomes et al., 2021). These satellite datasets are structured in a multi-dimensional  
278 array format, and provide layers of information across latitude and longitude (Open Data Cube, 2021).



279 Leveraging the growing availability of Analysis Ready Data (ARD), and with support from the  
280 Committee of Earth Observation Satellites (CEOS) (Killough, 2019), the ODC concept has been  
281 deployed in many countries across the world. These existing deployments include Digital Earth Africa  
282 (<https://www.digitalearthfranca.org/>), Digital Earth Australia (DEA) (<https://www.dea.ga.gov.au/>),  
283 Vietnam Open Data Cube (<http://datacube.vn/>), and Brazil Data Cube ([https://github.com/brazil-data-](https://github.com/brazil-data-cube)  
284 [cube](https://github.com/brazil-data-cube)), which provide various time-series datasets of the changing landscape and water content in  
285 these specific regions (Giuliani et al., 2020; Gomes et al., 2021; Killough, 2019; Lewis et al., 2017). The  
286 ecosystem and architecture of ODC is well explained at [opendatacube.org](http://opendatacube.org). The codes and tools used  
287 in this application drew upon the information provided in various DEA notebooks (Krause et al. (2021),  
288 which can be found at <https://github.com/GeoscienceAustralia/dea-notebooks/>.

## 289 2.5 Computation of river discharge

290 Derivation of river discharge ( $\text{m}^3/\text{s}$ ) was computed using total precipitation estimates (mm) over each  
291 river basin, and multiplied by a surface discharge runoff factor for the studied region (Sim et al., 2020).  
292 The surface runoff was estimated to be 60 % of total precipitation (Staub et al., 2000; Whitmore,  
293 1984). Precipitation data were extracted from the monthly NASA Global Precipitation Measurement  
294 (GPM) Level 3 IMERG dataset (<https://gpm.nasa.gov/data/imerg>). In this study, the Rajang river basin,  
295 as well as the combined basins of the Lupar, Sadong, and Saribas rivers (hereafter referred to as the  
296 Lupar basin), were studied for their river discharge rates in relation to TSS release.

Please provide some information about this study area. What is the land use and current situation in this basin

297  
298  
299  
300  
301  
302



303 3.0 Results & Discussion

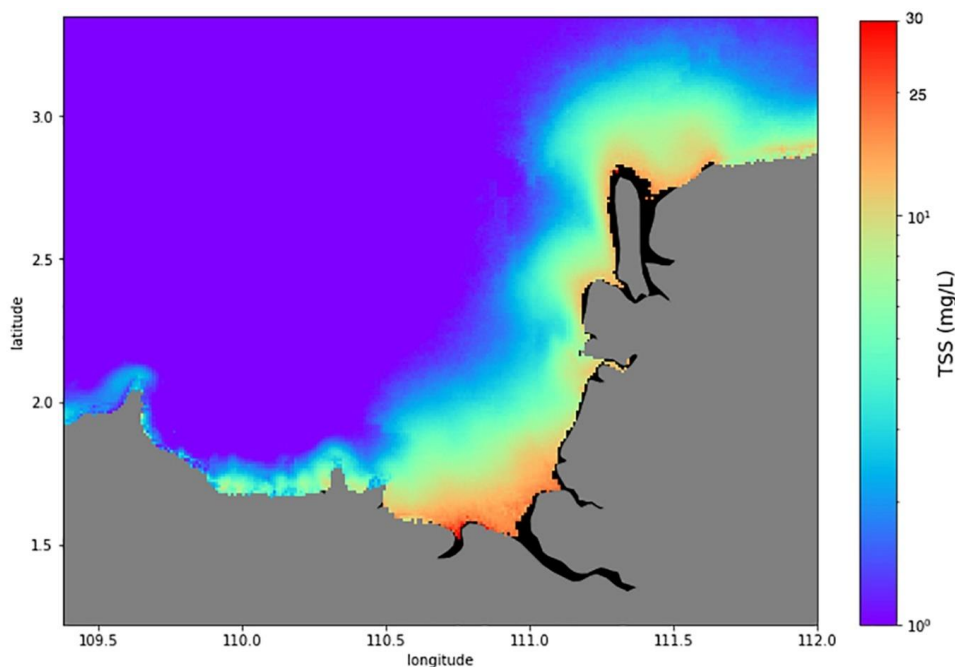
304 3.1 Spatial variation of TSS distribution

305 Changes in TSS distribution occur across space and time. The regional TSS remote sensing model  
306 calibrated in this study was applied to the time series of MODIS-Aqua data to study the variability of  
307 spatial TSS distribution and identify potential hotspot areas susceptible to TSS water quality  
308 degradation. The map of average TSS for the Sarawak region was generated (Eq. 2) by averaging all  
309 the daily MODIS-Aqua TSS images (2003 to 2019) and is presented in Fig. 5. The results show that the  
310 waters in the northeast of the study area, stretching from the Sadong river to the Rajang/Igan river  
311 have seen sustained levels of TSS over the 17 years considered in this study.

312 The temporally average spatial distribution map (Fig. 5) shows TSS concentrations in the range of 15  
313 – 20 mg/L near the river mouth areas, with widespread TSS plumes extending into the South China  
314 Sea (Fig. 5). Based on the Malaysia Marine Water Quality Criteria and Standard (Supplementary  
315 Materials, Table S2) (Department of Environment, 2019), these coastal waters fall under Class 1 in  
316 relation to their TSS (mg/L) status. This classification indicates that these coastal waters support and  
317 preserve marine life in this local region. Yet, several studies have expressed concerns regarding high  
318 TSS loadings in riverine waters owing to the impacts of various land use and land cover changes (LULC)  
319 (Ling et al., 2016; Tawan et al., 2020). Among these, the Rajang river has been highlighted to be heavily  
320 impacted by various LULC activities such as large-scale deforestation and construction of hydropower  
321 dams (Alamgir et al., 2020). In situ water quality studies by Ling et al. (2016) reported on high TSS  
322 estimates at one of the upstream tributaries of Rajang river, the Baleh river, with TSS readings up to  
323 approximately 100 mg/L. Another study by Tawan et al. (2020) reported a significant TSS release  
324 reaching to 940,000 mg per day during wet seasons, with maximum TSS concentrations of 1700 mg/L  
325 in the upstream tributaries of the Rajang river, particularly at the Baleh and Pelagus rivers. The  
326 majority of the upstream tributary rivers were categorised as Class II (during dry season) and Class III  
327 (during wet season) waters according to the National Water Quality Index (Supplementary Materials,



328 Table S3) (Department of Environment, 2014), due to increased soil erosion from surrounding LULC  
329 activities (Tawan et al., 2020). These local in situ findings provide valuable insights on point source TSS  
330 estimates in these LULC change regions. Coupled with our spatial map of average TSS captured by  
331 remote sensing technologies, our findings seem to suggest that a large portion of TSS loadings from  
332 inland and upstream rivers would have settled and deposited in these river channels and were not  
333 completely discharged outwards into the coastal areas, which would have caused major water quality  
334 degradation in the corresponding coastal systems.



335

336 Fig. 5: Temporally averaged 2°x 2° map of TSS distribution (on a log scale) across the time dimension for each pixel.

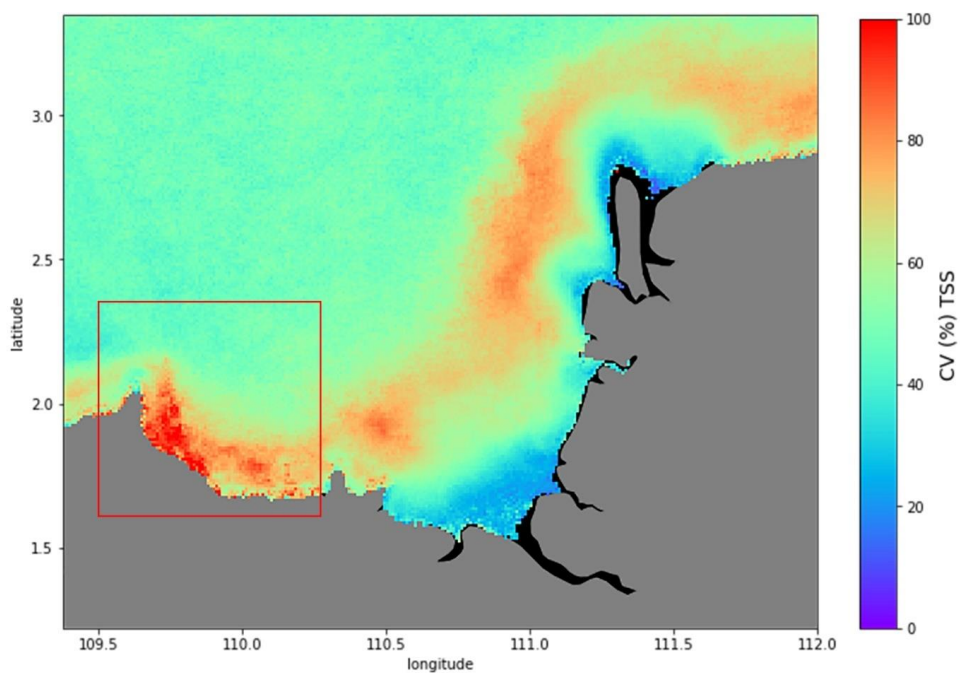
337 Historical patterns of TSS concentration were assessed by comparing annual maps of average TSS  
338 distribution (Supplementary Materials; Fig. S1), as well as time series of TSS estimates at the Lupar  
339 and Rajang river mouths (Supplementary materials; Fig. S2). From our findings, the annual TSS maps  
340 further support the observation where TSS release was evident at Lupar and Rajang/Igan river mouths  
341 from 2003 till 2019, which points to Class I of local water quality standards in relation to TSS (mg/L)



342 status. This was found to consistently occur every year. Furthermore, the TSS trend study showed that  
343 both the Lupar and Rajang river mouth points have a gradual increase of TSS concentration over the  
344 17 years (Supplementary materials; Fig. S2). This increasing trend was, however, not statistically  
345 significant ( $p = 0.43$  for Lupar, and  $p = 0.15$  for Rajang).

346 Moreover, a map of the TSS coefficient of variation (CV) was computed to identify areas with a high  
347 degree of relative TSS variation over time (Fig. 6). Here again, the map of CV (%) was produced by  
348 aggregation of the daily MODIS-Aqua images (6192 time steps) from 2003 until 2019. Figure 6 shows  
349 that the Samunsam-Sematan coastal region (as highlighted by the red box) exhibits an increased level  
350 of TSS distribution variability, with a recorded CV of more than 90 %.

351 The Samunsam-Sematan coastal region contains near-pristine mangrove forests which are sheltered  
352 from major LULC activities, as compared to other studied sites. Samunsam-Sematan is also well-known  
353 locally as a recreational hotspot with coral reefs and various national parks (Sarawak Tourism Board,  
354 2021). Data from the Centre for International Forestry Research (CIFOR) Forrester Carbon database  
355 (CIFOR, n.d.) revealed that there was more than double the amount of total forest loss (approx. 5,000  
356 Ha) recorded in Lundu, a nearby township in the Sematan area in 2011 as compared to the previous  
357 years. Deforestation activities, regardless of their scale, can inevitably promote sediment loss and soil  
358 leaching into the nearby river systems (Yang et al., 2002). Important information regarding the  
359 variability in water quality (as shown in Fig. 6) can provide support to local authorities and relevant  
360 agencies in order to identify vulnerable areas that need to be monitored closely, such as the Lundu-  
361 Sematan region in this case. The CV map thus offers interesting insights into how TSS distribution can  
362 vary across large spatial areas, which can ultimately impact local socio-economic activities in this  
363 region (Lee et al., 2020b).



364

365 Fig. 6: Map of CV (%) calculated from the daily time series of MODIS-Aqua satellite images from 2003 until 2019.

366

367

368

369

370

371

372

373

374

375



376 3.2 Temporal variation of TSS distribution

377 On a temporal scale, the northeast (NE) monsoon period shows a distinct difference in the widespread  
378 intensity of TSS distribution as compared to the southwest (SW) monsoon period, along the Sarawak  
379 coastline over the 17 years of the considered time series (Fig. 7). Mapping of temporal variations  
380 between monsoons using time-series MODIS-Aqua datasets can provide an improved understanding  
381 on the intensity of monsoonal patterns in driving the TSS distribution in this region. As shown in Figure  
382 7, TSS release can be seen to extend further into the open ocean South China Sea region during the  
383 NE monsoon periods (Fig. 7a) in comparison to the SW monsoon periods (Fig. 7b).

384 In addition, the differences in TSS release between the NE and SW monsoons  $((NE-SW)/NE \times 100)$  were  
385 mapped as shown in Fig. 7c. Widespread TSS plumes are detected at Lundu/Sematan region (>80 %  
386 relative difference in TSS concentration) on the southwest side of the study area, while substantial  
387 TSS plumes are observed in front of the Igan river channel, with more than 50 % relative difference in  
388 TSS concentration in comparison to SW monsoon periods. Sadong coastal area is observed to receive  
389 considerable TSS loadings (> 30%) during NE monsoon periods.

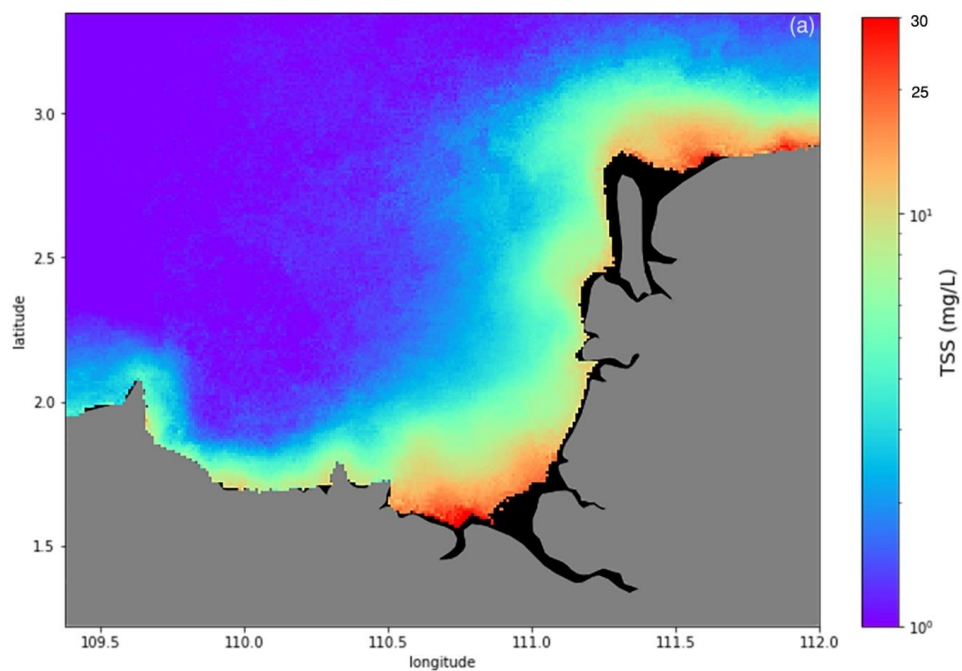
390 These coastal areas would thus be more likely to be impacted by the TSS release during the NE  
391 monsoon periods. These findings further strengthen the evidence that tropical rivers are majorly  
392 impacted by climatic variability such as monsoonal patterns, as highlighted in a study at Baleh river in  
393 Sarawak (Chong et al., 2021). This suggests that monsoon rains, which typically last for several months,  
394 play an integral role in driving the discharge of TSS in tropical rivers.

395

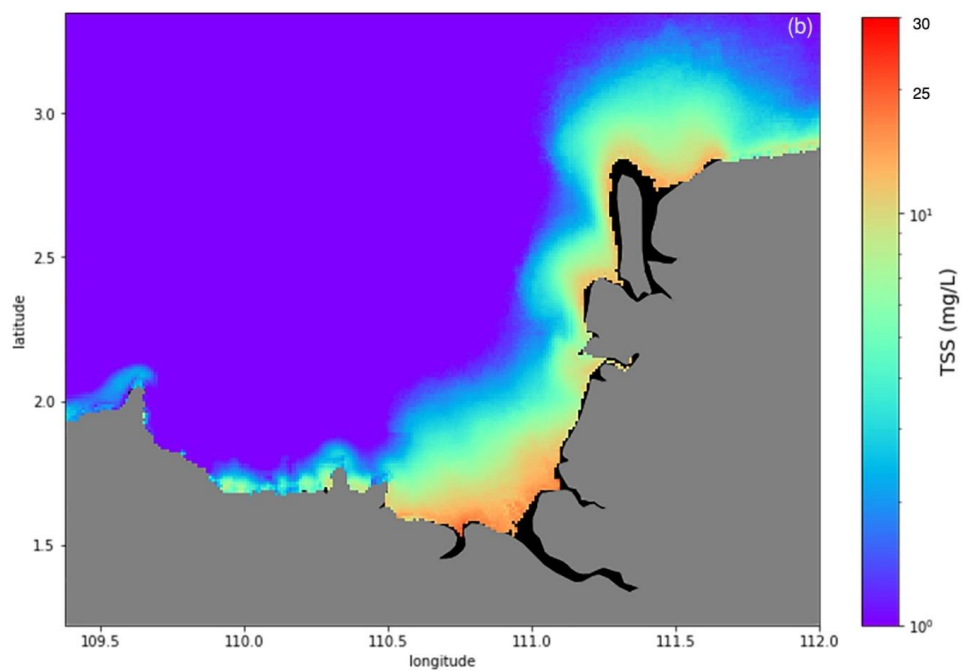
396

397

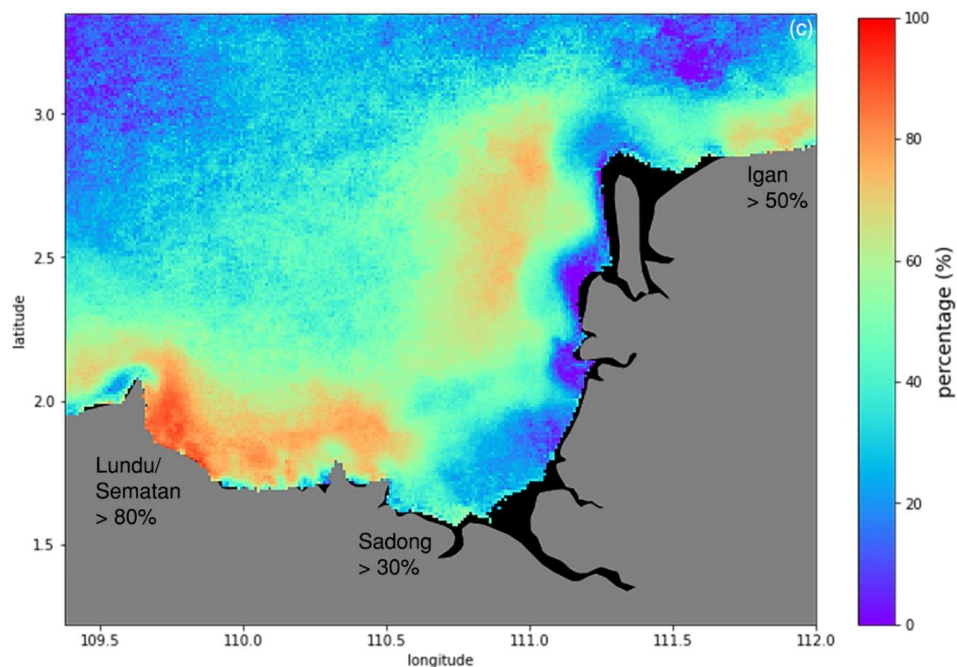
398



399



400



401

402 Fig. 7: Long-term average of TSS estimates (mg/L) during the Northeast monsoon (a), and the Southwest monsoon (b). The  
403 map of TSS difference between the Northeast and Southwest monsoon periods, computed in relative percentage (%), is  
404 shown in (c).

405 Several climatic studies in the Borneo region highlighted 2009 as a year with extreme rainfall events  
406 which caused major floods in Sarawak (Dindang et al., 2011; Sa'adi et al., 2017), while drought events  
407 were reported in 2014 (Bong and Richard, 2020). Hence, in this study, TSS dynamics for the Lupar and  
408 Rajang rivers were studied by assessing the variation of TSS values at selected pixels in relation to  
409 monsoonal rainfall patterns in 2009 and 2014 (Supplementary Materials; Fig. S3).

410 Monthly precipitation values (mm) over the Lupar and Rajang basins were extracted from the Global  
411 Precipitation Measurement (GPM) satellite datasets (Supplementary Materials, Fig. S4 - 7) in order to  
412 assess the influence of precipitation in each river basin in relation to TSS concentration at the  
413 corresponding river mouth.

414 Generally, the results show fluctuations of TSS concentrations across the NE and SW monsoon periods  
415 in relation to precipitation values (Fig. 8a – d). Based on Fig. 8a, monthly precipitation values recorded



416 for the Lupar river basin in 2009 showed a clear decreasing trend from the NE monsoon period (wet  
417 season) to the SW monsoon period (dry season), while gradually increasing approaching the year end's  
418 NE monsoonal period. A similar precipitation pattern was observed for the Rajang river basin during  
419 the same year (Fig. 8c).

420 However, these results also show that the TSS distribution (mg/L) at the Lupar river mouth seems to  
421 show no distinct trend of decreasing TSS concentration estimates during the SW monsoon period in  
422 year 2009 (Fig. 8a) in relation to its precipitation values. Additionally, a sharp rise of TSS release can  
423 be seen in the month of May (beginning of SW monsoon period), with a near equivalent intensity of  
424 TSS release during the NE monsoon period. This observation may potentially be caused by the lag  
425 between the time of rainfall events occurring during NE monsoon periods and TSS release entering  
426 the coastal river regions. A similar observation was described by Sun et al. (2017a) suggesting that  
427 riverine outputs could take several days, and even up to one month to reach the coastal river points.  
428 Considering the occurrence of extreme rainfall events in 2009, our findings are in agreement with  
429 these processes as TSS concentrations generally exhibit a similar intensity throughout the NE and SW  
430 monsoonal periods for the Lupar river (Fig. 8a). This result could suggest that the occurrence of  
431 extreme rainfall events, as reported for the year 2009, can exert a much larger impact on TSS  
432 transportation and release in monsoon-driven tropical rivers.

433 However, our estimates show a generally lower TSS concentration at the Rajang river mouth during  
434 the SW monsoon periods (dry season) in 2009 (Fig. 8c) as compared to the Lupar river mouth (Fig. 8a).  
435 While these observations were recorded during the same year in 2009, when Sarawak experienced  
436 extreme rainfall events, the monsoonal influence between these two different river basins show a  
437 slight difference in terms of TSS distribution. A possible reason for these observations can be explained  
438 by the Rajang river's unique meandering features, which can potentially induce a different  
439 sedimentological behaviour compared to the Lupar river channels, which was discussed by Omorinoye

Is there any data for the rainfall event related to monsoon season?



440 et al. (2021) in a study on geomorphological features of the Sadong river in relation to the  
441 sedimentation process.

442 Drought events in 2014 can be seen to impact the precipitation values at both the Lupar (Fig. 8b) and  
443 Rajang river basins (Fig. 8d). There is no apparent patterns of decreasing precipitation values during  
444 the shift of NE to SW monsoonal periods as compared to the year 2009, for either river basin. However,  
445 precipitation values were found to increase sharply during the year end NE monsoon period for both  
446 river basins. The TSS concentrations at the Lupar coastal river points were found to be the highest  
447 during the NE monsoon period earlier in January and February of 2014 (Fig. 8b). This may be due to  
448 the temporal lag in the transition of TSS discharge into the coastal systems arising from the prior  
449 months (November and December) in the previous year, when higher rainfall events were typically  
450 observed in this region (Gomyo and Koichiro, 2009; Tangang et al., 2012). The TSS distribution at both  
451 Lupar and Rajang coastal river points showed no distinct trend in relation to the precipitation values  
452 throughout a period of ten months until November 2014. These findings suggest that coastal areas in  
453 the Borneo region may not be experiencing critical water quality degradation during dry seasons.

454

455

456

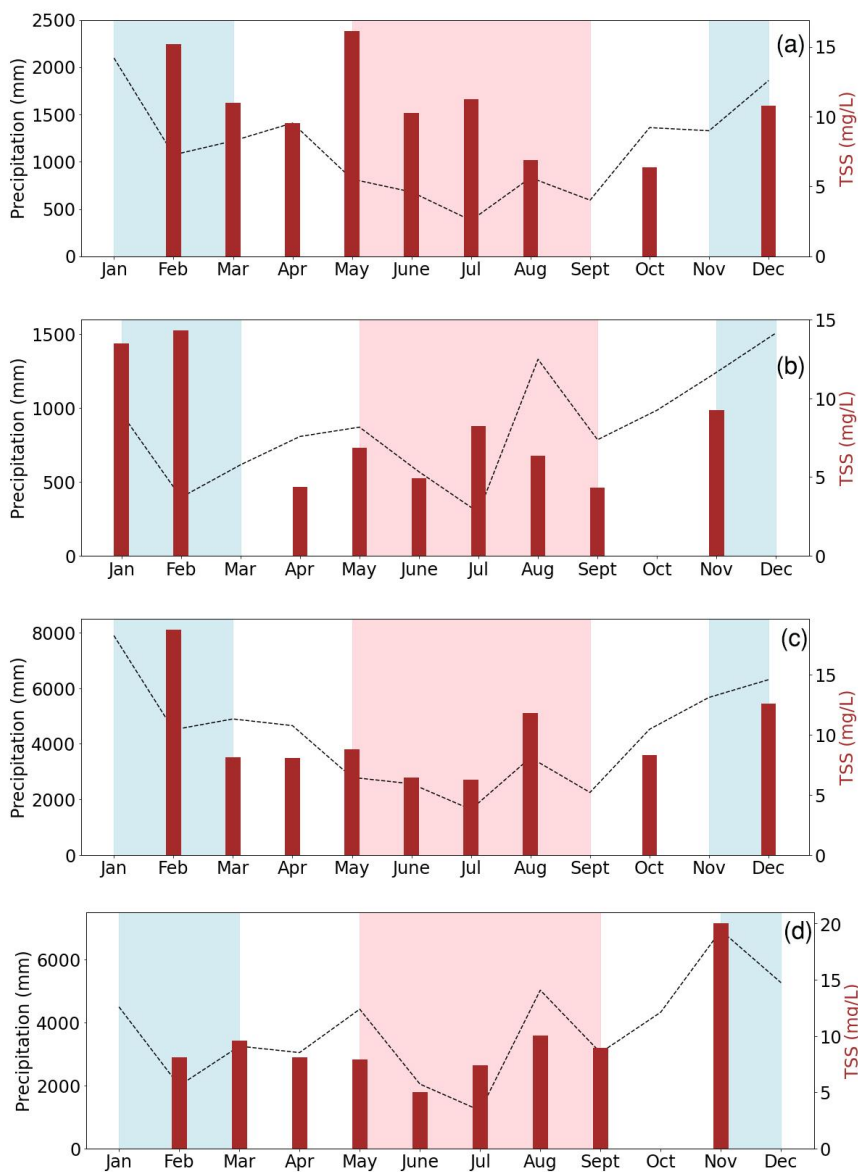
457

458

459

460

461



462

463 Fig. 8: Temporal analysis of precipitation (mm) from the Lupar and Rajang river basins in relation to TSS concentrations (mg/L)  
464 during the NE and SW monsoon periods at the Lupar ((a): 2009; (c): 2014) and Rajang ((b): 2009; (d): 2014) coastal river point.  
465 The NE monsoon months are highlighted with a blue background; those of the SW monsoon with a pink background, and  
466 intermonsoon periods with a white background.



467 Considering the temporal variation recorded across monsoons, maps of relative TSS anomalies were  
468 calculated for each year as the difference with respect to the long-term TSS mean (Fig. 5), in order to  
469 detect changes of TSS distribution occurring annually (Fig. 9). As shown in Figure 9, year 2010  
470 experienced a distinct increase of TSS distribution (approximately 100 %), with widespread pattern  
471 extending into open ocean waters, in comparison to the long-term TSS mean. This finding provides an  
472 interesting insight into the effects of extreme rainfall events as recorded in year 2009, which could  
473 potentially intensify TSS release into the coastal and open ocean waters. The effects of TSS release  
474 can still be seen a year after the extreme rainfall events in this region. This observation could provide  
475 further evidence that the impacts of the TSS release from the land into rivers and coastal systems may  
476 only take effect after a substantial period, as previously observed by Sun et al. (2017a).

477 Figure 9 further reveals an interesting pattern of TSS increase in the Samunsam-Sematan region from  
478 year 2004 until 2019, with exceptions during the years 2007 and 2008. As previously highlighted in  
479 Section 3.1, the Samunsam-Sematan region has been observed to be a vulnerable coastal area with  
480 respect to TSS water quality degradation. From the annual map of TSS anomalies (Fig. 9), we can see  
481 that the TSS distribution has the tendency to accumulate in the Samunsam-Sematan region, as  
482 opposed to being distributed into the open ocean waters. This may be due to the geographical and  
483 hydrological characteristics of these coastal regions (Martin et al., 2018), as the TSS release may be  
484 sheltered from open ocean waters, and hence induce a higher TSS accumulation in these coastal  
485 regions.

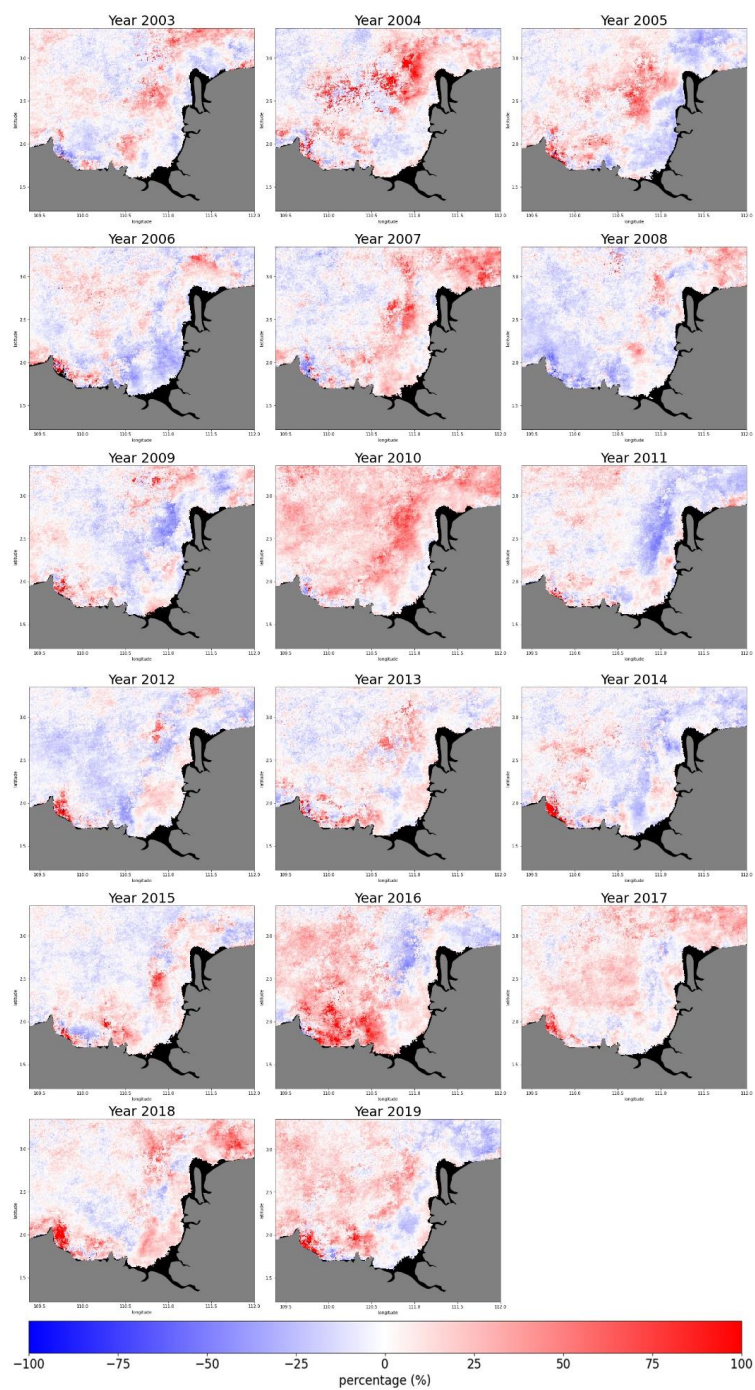
486

487

488

489

490



491

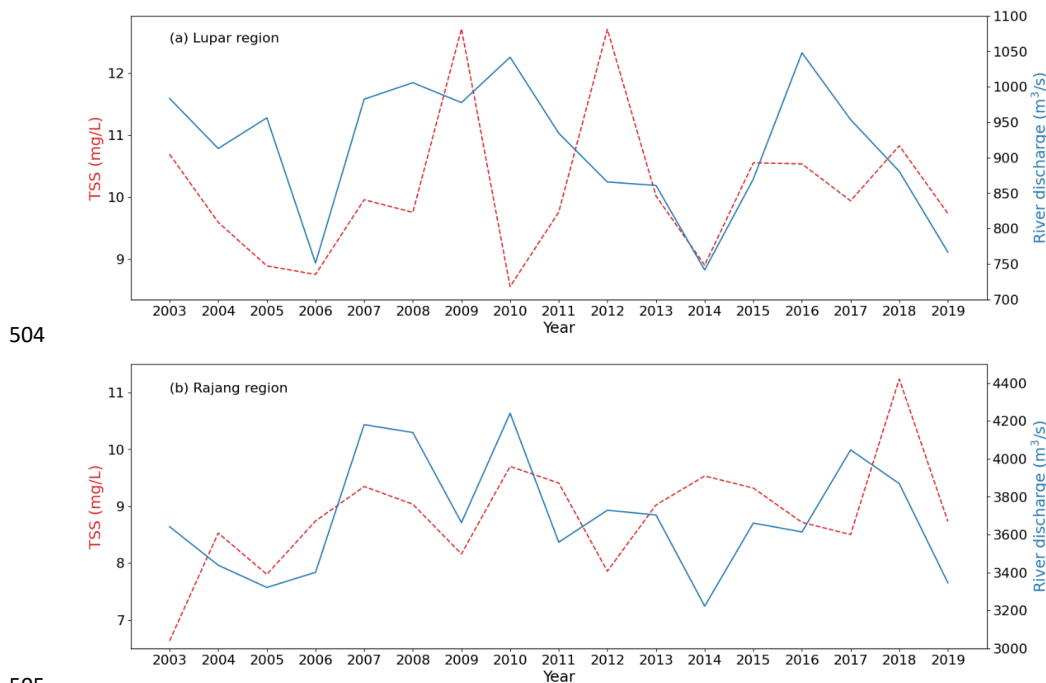
492 Fig. 9: Map of relative TSS distribution anomalies with respect to the long-term mean, represented as percentage (%), from  
493 year 2003 until 2019.



494 3.3 Hydrological factors driving TSS discharge

495 Apart from the influence of monsoonal patterns, hydrological factors such as the river discharge are  
496 among the dominant drivers in transporting various water constituents in riverine and coastal systems  
497 (Loisel et al., 2014; Petus et al., 2014; Sun, 2017b; Verschelling et al., 2017). In this study, river  
498 discharge from the Lupar and Rajang basins was estimated and investigated.

499 Yearly river discharge estimates from 2003 until 2019 were investigated to assess its effect on the TSS  
500 distribution (Fig. 10) represented by changes in TSS values for pixels located at each Lupar and Rajang  
501 coastal river points (Supplementary Materials, Fig. S3). Figure 10a shows that river discharge values in  
502 the Lupar basin (750 to 1050 m<sup>3</sup>/s) are approximately twice lower than the Rajang river discharge (Fig.  
503 10b), which recorded a range of 3,200 to 4,000 m<sup>3</sup>/s.



506 Fig. 10: Time-series analysis of river discharge (m<sup>3</sup>/s) in relation to TSS concentrations (mg/L) for the Lupar (a) and Rajang (b)  
507 basins from year 2003 to 2019. Note the differing scaling on the ordinate axes in each plot.



508 From **our findings**, discrepancies between TSS estimates and river discharge were identified in both  
509 the Lupar and Rajang coastal regions in these annual time-series, where river discharge was inversely  
510 correlated with TSS estimates. These discrepancies are not uncommon, as previously highlighted in a  
511 study by Zhan et al. (2019). Especially in 2010 for the Lupar river, Fig. 10a shows a drop in TSS release  
512 in relation to the steady increase of river discharge from the river basin. In 2011 and 2012, a negative  
513 correlation can be seen between river discharge and TSS estimates, while in subsequent years from  
514 2013 until 2015, there is a clear positive correlation. Although there is no obvious environmental  
515 factor that would explain these discrepancies, these findings may imply a complex interaction  
516 between human interventions, such as damming and deforestation activities, as well as varying  
517 hydrological and atmospheric conditions (wind and tidal mixing) in regulating TSS dynamics (Wu et al.,  
518 2012; Zhan et al., 2019).

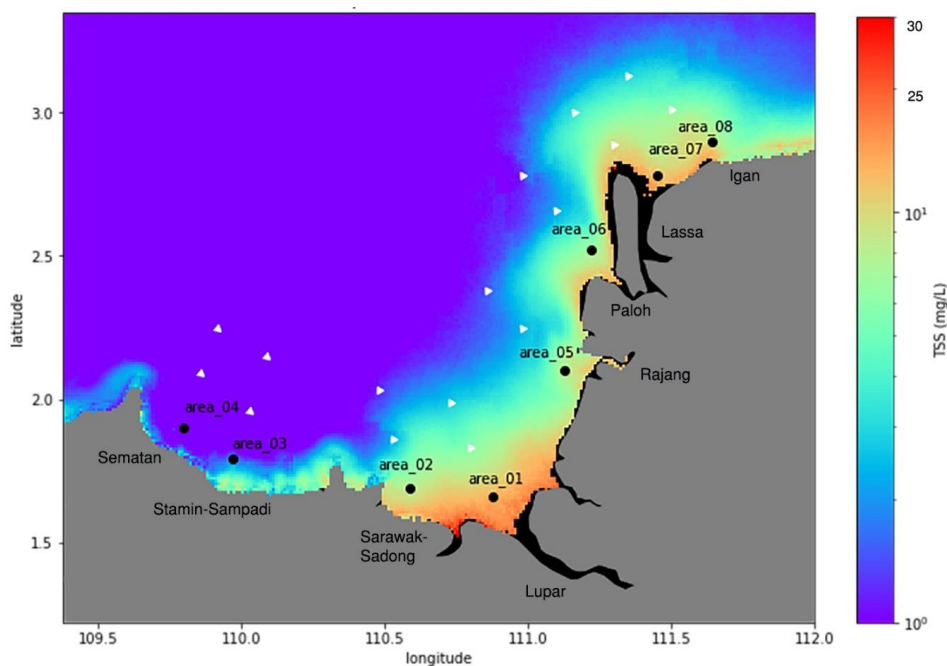
519 The correlation between TSS release and river discharge at both the Lupar and Rajang coastal areas  
520 was further evaluated in this study. Even though river discharge has been shown (in other global  
521 studies) to be one of the dominant factors in moderating TSS release (Fabricius et al., 2016; Tilburg et  
522 al., 2015; Verschelling et al., 2017; Wu et al., 2012), the TSS distribution at both the Lupar and Rajang  
523 river mouths in this study can be seen to be only poorly correlated with river discharge from each river  
524 basin (Supplementary Materials, Fig. S8a and b). The TSS output from the Lupar basin recorded a  
525 correlation coefficient of  $r = 0.15$ , while river discharge from the Rajang basin did not substantially  
526 influence the TSS release either, with  $r = 0.27$  throughout the seasons. Coupled with tidal mixing  
527 processes (Ramaswamy et al., 2004; Zhou et al., 2020), it is possible that human activities such as  
528 deforestation, logging, and construction of dams, which are largely occurring within the Rajang basin  
529 (Alamgir et al., 2020), are mainly driving TSS release and resuspension in this area. This indicates that  
530 although TSS release is regarded to be highly dependent on, and controlled by river discharge patterns,  
531 this interaction often represents an intricate process linked to local hydrodynamics process and socio-  
532 economic conditions (Espinoza Villar et al., 2013; Fabricius et al., 2016; Valerio et al., 2018; Zhan et al.,  
533 2019).



534 3.4 Variability of TSS across coastal waters

535 As previously observed in Fig. 5, varying river plumes of TSS were evidently detected within the coastal  
536 regions of the study area. Notably, coastal river plumes represent important factors driving the  
537 transport of water constituents and nutrients from coastlines to the open oceanic systems (Petus et  
538 al., 2014). To assess this and evaluate the water quality status in coastal zones, the spatial extent of  
539 TSS release was investigated along transects covering the territorial (12 nautical miles) and open water  
540 areas (24 nautical miles) of the Sarawak region (Fig. 11).

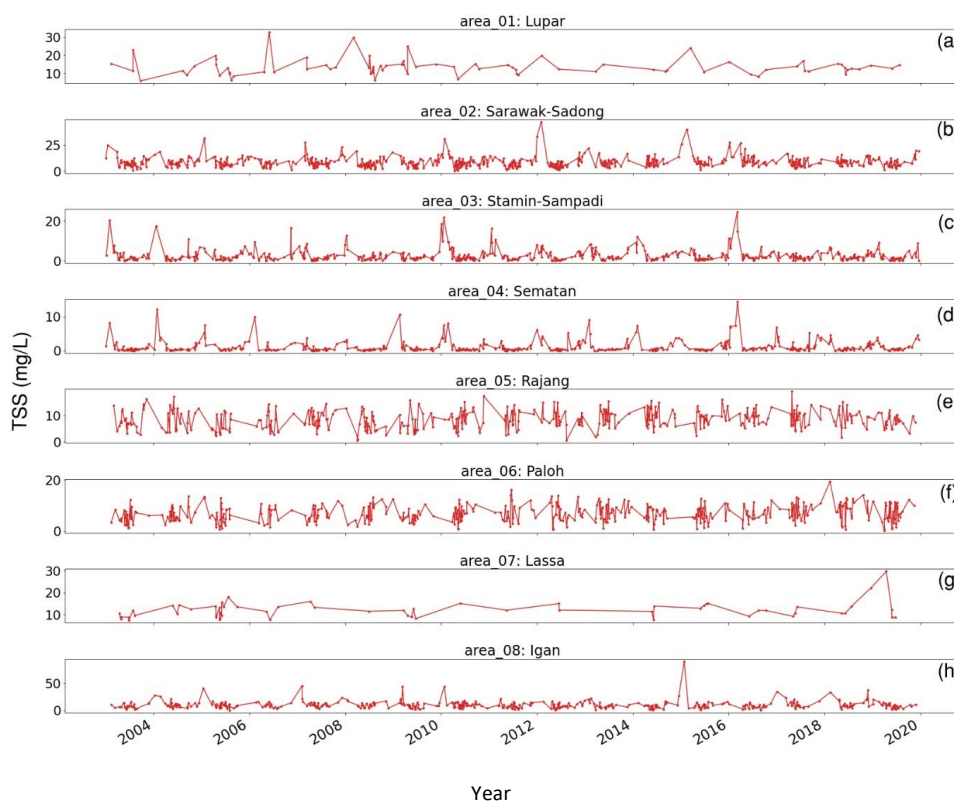
541 A total of eight coastal points were selected based on the main river mouths located in the southwest  
542 region of Sarawak. Transect points are positioned in a line starting at the coastal river points to  
543 examine the variations of TSS distribution across different water zones. Daily changes in TSS  
544 concentration for each pixel located in front of the river mouths were plotted from 2003 until 2019  
545 (Fig. 12).



546



547 Fig. 11: Map of average TSS estimates (mg/L) with indicators at eight main river mouths and their transect, extending from  
548 coastal waters into territorial and open ocean systems. Indicators of each river mouths are as follows: area\_01 – Lupar river;  
549 area\_02 – Sarawak-Sadong river; area\_03 - Stamin-Sampadi river i; area\_04 – Sematan river; area\_05: Rajang river; area\_06:  
550 Paloh river; area\_07: Lassa river; and area\_08: Igan river).



551  
552 Fig. 12: Graphs of daily TSS estimates (mg/L) recorded at eight river mouth points from 2003 to 2019. Presentation of each  
553 river mouths is as follows: a) area\_01; b) area\_02; c) area\_03; d) area\_04; e) area\_05; f) area\_06; g) area\_07; h) area\_08.  
554 Note the different TSS scales in each plot.

555 From the high temporal resolution graphs in Fig. 12, no general trend of TSS concentration can be  
556 identified over the years at each coastal point. It is worth highlighting that the daily temporal  
557 resolution was particularly affected at coastal points located in front of the Lupar (area\_01) and Lassa  
558 (area\_07) river mouths due to various pixel data quality issues in these areas. Nonetheless, more than  
559 80 satellite images with minimum cloud coverage at these two locations were processed, while the  
560 remaining coastal points had a total of more than 400 satellite images to assess the temporal trend.



561 Despite the fact that no distinct upward or downward trend was observed, our findings indicate that  
562 several river mouths are actively discharging and accumulating substantial TSS amounts over the  
563 period of years, while resuspension of bottom sediments induced by wind and tidal cycle is another  
564 factor contributing to the variation of TSS values (Park, 2007; Song et al., 2020).

565 The coastal region of the Sarawak-Sadong river (area\_02) shows relatively high TSS distribution  
566 patterns with some periods recording an estimate of over 30 mg/L of TSS concentration. This is in  
567 agreement with the localised characteristics of the Sarawak river basin which essentially drains  
568 through the populated Kuching area with high industrial and development activities in the capital city  
569 of Sarawak (DID, 2021b). In comparison with other river mouth points, a steady TSS concentration  
570 below 20 mg/L was recorded across the Stamin-Sampadi (area\_03), Sematan (area\_04), Rajang  
571 (area\_05), and Paloh (area\_06) river mouths. Consistently high TSS values in the daily plots were  
572 recorded at the Lupar (area\_01) and Pulau Bruit-Lassa (area\_07) river mouths, with estimates of up to  
573 30 mg/L on a near-daily basis. Similar high TSS amounts from the Igan (area\_08) river mouth, situated  
574 northeast side of the Pulau Bruit-Lassa region, were observed in Cherukuru et al. (2021) and Staub et  
575 al. (2000).

576 Although the daily TSS estimates at each river point are in line with various reported studies (Chen et  
577 al., 2011, 2015b; Kim et al., 2017; Mungen et al., 2020; Zhang et al., 2010a), these estimates can be  
578 expected to be much higher for sampling points much closer to the river mouths. The selection of  
579 coastal river points in this study was made to minimize the gaps with respect to various pixel data  
580 quality issues in the MODIS-Aqua datasets, and hence, the use of coastal river points closer to shore  
581 would have been impractical.

582 These findings further suggest that higher TSS loadings within the coastal river areas would have been  
583 diluted or deposited while travelling to the open oceanic systems as they are weakly impacted by river  
584 discharge in relation to offshore distance (Espinoza Villar et al., 2013). This understanding can be  
585 observed in Fig. 13, which shows a progressively decreasing TSS estimates at each transect in relation



586 to the distance from the shore. Generally, TSS estimates in coastal zones (first transect point) show  
587 considerably higher TSS concentrations. When moving outwards to territorial waters (second transect  
588 point), TSS concentration estimates decrease by nearly 50 % before travelling to open ocean systems  
589 (third transect point), except for the northeast regions (area\_07 and area\_08) which seem to show  
590 large extension of TSS plumes to the open ocean waters, as also highlighted by Cherukuru et al. (2021).  
591 A reversed trend can be seen in the plot corresponding to the Sematan coastal river systems, although  
592 the absolute increase in TSS estimates across water zones (0.2 mg/L in total) here is only marginal (Fig.  
593 15d).

594 Nonetheless, it is important to present these synoptic findings to address existing water quality  
595 practices and regulations implemented in this local region, in order to improve the monitoring and  
596 management of its coastal systems. According to the Malaysia Marine Water Quality Criteria and  
597 Standard (Supplementary Materials, Table S2), the coastal areas of Sarawak are dominantly  
598 categorised as Class I quality. Our findings in the southwest coastal areas (Sematan and Stamin-  
599 Sampadi) showed that the coral reefs there can be well-maintained with negligible impacts from TSS  
600 loadings (Fig. 11). While these Sematan and Stamin-Sampadi coasts can be seen to be in a healthy  
601 water quality state (low average TSS concentration, see e.g. Fig 11), the high coefficient variation  
602 reported in these coastal waters, as previously highlighted in Section 3.1 (Fig. 6), clearly stresses the  
603 importance of understanding how the quality of coastal systems can vary and be affected by human  
604 intervention and changing landscapes over time.

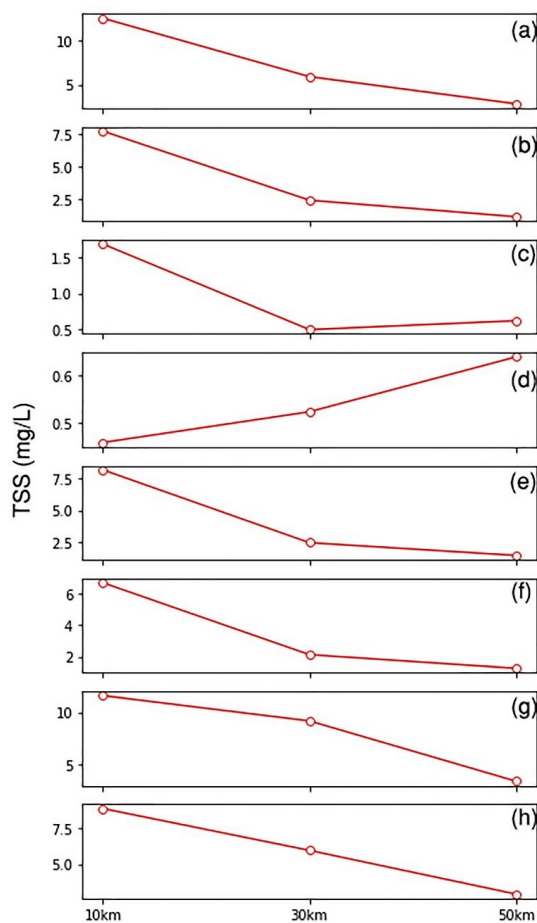
605

606

607

608

609



610

611 Fig. 13: Average TSS estimates (mg/L) computed from 2003 to 2019 for each of the eight rivers (area\_01: (a), area\_02: (b);  
612 area\_03: (c); area\_04: (d); area\_05: (e); area\_06: (f); area\_07: (g); and area\_08: (h)) and their relevant transect points with  
613 distance of 10 km (coastal waters), 30 km (territorial waters) and 50 km (open ocean waters) from the shoreline. Note the  
614 varying TSS scales on the ordinate axes in each plot.

615

616

617

618



619 3.5 Discussion of TSS implications for coastal waters

620 High discharge of TSS into coastal environments can lead to adverse environmental and ecological  
621 implications. The presence of TSS affects water transparency and light availability within the surface  
622 waters (Dogliotti et al., 2015; Nazirova et al., 2021; Wang et al., 2021). Among others, TSS affects the  
623 photosynthesis activities of algae and macrophytes. TSS in water creates a reduction in light  
624 penetration, which impacts the primary production of aquatic organisms and hence the support  
625 system of marine life (Bilotta and Brazier, 2008; Loisel et al., 2014).

626 Additionally, TSS exerts an influence on zooplankton communities. Reduction in water clarity induces  
627 changes in the zooplankton's biomass volume and composition, while TSS may carry a level of toxicity  
628 which affects zooplankton through ingestion (Chapman et al., 2017; Donohue and Garcia Molinos,  
629 2009). Apart from that, accumulation and deposition of sediments decreases the level of dissolved  
630 oxygen (DO) at the bottom of the water column, and subsequently impacts the benthic invertebrate  
631 groups (Chapman et al., 2017). Moreover, substantial TSS deposition tends to cause harmful physical  
632 effects to these benthic groups, such as abrasion, and even clogging by sediment particles (Chapman  
633 et al., 2017; Langer, 1980).

634 As a result of these TSS effects on lower trophic levels, fish communities are critically impacted, with  
635 a reduction in diversity and abundance (Kemp et al., 2011). While fish communities learn to adapt to  
636 a range of TSS loads (Macklin et al., 2010), increase of TSS concentrations often depletes DO  
637 concentrations in the water system and causes stress towards these aquatic communities (Henley et  
638 al., 2000). Fish populations tend to decrease, as feeding and growth rates are negatively impacted  
639 (Shaw and Richardson, 2001; Sutherland and Meyer, 2007).

640 Threats to coral reefs have been linked to sediment-induced stress which often leads to a reduction  
641 in the coral's growth and metabolic rate, as well as impending mortality (Erftemeijer et al., 2012;  
642 Gilmour et al., 2006; Risk and Edinger, 2011). Factors of coral stress are driven by nutrient-rich  
643 sediments and microbes which are being carried by TSS, with impacts on the health of coral tissues



644 (Hodgson, 1990; Risk and Edinger, 2011; Weber et al., 2006). A reduction in light availability impede  
645 the development of corals (Anthony and Hoegh-Guldberg, 2003; Rogers, 1979; Telesnicki and  
646 Goldberg, 1995). A combined increase in TSS and nutrient loadings contribute to the decrease of coral  
647 species diversity and composition (Fabricius, 2005).

648 Essentially, presence of TSS in water systems has impacts across various aquatic biota. With the severe  
649 implications of decreased fish population, this could lead to a disruption of fisheries activities by local  
650 communities, especially considering that more than 80 % of the Sarawak population is living in the  
651 coastal areas (DID, 2021a). Coral reefs are important coastal biodiversity assets to the Sarawak region,  
652 especially around the Talang-Talang and Satang islands on the southwest coast of Sarawak (Long,  
653 2014). With the use of remote sensing technologies in monitoring Sarawak coastal water quality, the  
654 approach presented in this paper provides digital-based solutions to assist relevant authorities and  
655 local agencies to better manage the Sarawak coastal waters and their resources.

656

657

658

659

660

661

662

663

664

665

666

667

668

669



670 4.0 Conclusion

671 In this study, a regional empirical TSS retrieval model was developed to analyse TSS dynamics along  
672 the southwest coast of Sarawak. The empirical relationship between in situ reflectance values,  $Rrs(\lambda)$ ,  
673 and in situ TSS concentrations was established using a green-to-red band ratio using the MODIS-Aqua  
674  $Rrs(530)$  and  $Rrs(666)$  reflectance bands. An evaluation of the TSS retrieval model was carried out with  
675 error metric assessment, which yielded results of bias = 1.0, MAE = 1.47 and RMSE = 0.22 in mg/L  
676 computed in log<sub>10</sub>-transformed space prior to calculation. A statistical analysis using a k-fold cross  
677 validation technique ( $k = 7$ ) reported a low error metrics (RMSE = 0.2159, MAE = 0.1747).

678 The spatial TSS distribution map shows widespread TSS plumes detected particularly in the Lupar and  
679 Rajang coastal areas, with average TSS range of 15 – 20 mg/L estimated at these coastal areas. Based  
680 on the spatial map of the TSS coefficient of variation, large TSS variability was identified in the  
681 Samunsam-Sematan coastal areas ( $CV > 90\%$ ). The map of temporal variation of TSS distribution  
682 points to a strong monsoonal influence in driving TSS release, with large differences identified  
683 between the northeast and southwest monsoon periods in this region. From the annual TSS anomalies  
684 maps, the Samunsam-Sematan coastal areas demonstrated strong TSS variation spatially, while  
685 widespread TSS distribution with nearly 100 % of TSS increase in comparison to long term mean was  
686 observed in 2010. Furthermore, our study on river discharge in relation to TSS release demonstrated  
687 a weak relationship at both the Lupar and Rajang coastal river points. Study on the TSS variability  
688 across coastal river mouths implied that higher TSS loadings in the coastal areas are potentially being  
689 deposited or diluted in the process of being transported into the open ocean waters, with varying  
690 magnitude at several coastal river points.

691 Overall, these coastal zones remain within local water quality standards to support various marine and  
692 socio-economic activities in this region. However, it is important to highlight the various human  
693 activities that are widely ongoing in this region, which include deforestation and logging activities  
694 (Alamgir et al., 2020; Hon and Shibata, 2013; Vijith et al., 2018). Impacts from these activities in



695 Sarawak can potentially aggravate current soil erosion issues, and ultimately induce more soil leaching  
696 and runoff from land to water systems, especially during heavy rainfall events (Ling et al., 2016; Vijith  
697 et al., 2018). As a result, human activities may have a greater influence on driving riverine sediments  
698 than climatological factors, as reported by Song et al. (2016). As such, this work presents the first  
699 observation of TSS distributions at large spatial and temporal scales in Sarawak's coastal systems, and  
700 of the potential associated impacts on the South China Sea. The findings derived from this work can  
701 be used to support local authorities in assessing TSS water quality status in the coastal areas of  
702 concern, and to enhance coastal management and conservation strategies. The application of remote  
703 sensing technologies is of great benefit in the development of sustainable sediment management in  
704 the Sarawak coastal region, as demonstrated in this study.

705 Data availability. The dataset related to this study is available as supplement to this paper.

706 Author contributions. Conceptualization, J.C., N.C., E.L., and M.M.; Formal analysis, J.C., N.C. and E.L.;  
707 Funding acquisition, M.M, N.C., and A.M.; Investigation, J.C., N.C., E.L., M.P., P.M., A.M., and M.M.;  
708 Methodology, J.C., N.C., E.L., and M.M.; Resources, J.C., N.C., E.L., M.P., and M.M.; Validation, J.C.,  
709 N.C., E.L. and M.M.; Writing— original draft, J.C.; Writing—review & editing, J.C., N.C., E.L., P.M., and  
710 M.M.; Supervision, M.M., N.C., and A.M.; Project administration, M.M., A.M., and N.C.

711 Competing interests. The authors declare that they have no conflict of interest.

712 Acknowledgement. We thank Sarawak Forestry Department and Sarawak Biodiversity Centre for  
713 permission to conduct collaborative research in Sarawak under permit numbers NPW.907.4.4(Jld.14)-  
714 161, SBC-RA-0097-MM, and Park Permit WL83/2017. We would like to extend our gratitude to all the  
715 boatmen and crew during all the field expeditions. Special thanks to Pak Mat and Minhad during the  
716 western region sampling, and Captain Juble, as well as Lukas Chin, during the eastern region cruises.  
717 We are appreciative to members of AQUES MY for their kind participation and involvement, especially  
718 to Ashleen Tan, Jack Sim, Florina Richard, Faith Chaya, Edwin Sia, Faddrine Jang, Gonzalo Carrasco,  
719 Akhmetzada Kargazhanov, Noor Iskandar Noor Azhar, and Fakharuddin Muhamad. The study was



720 supported by Australian Academy of Sciences under the Regional Collaborations Programme, Sarawak  
721 Multimedia Authority (Sarawak Digital Centre of Excellence) and Swinburne University of Technology  
722 (Swinburne Research Studentship).

723

724

725

726

727

728

729

730

731

732

733

734

735

736

737

738

739

740

741

742

743

744

745

746

747

748

749

750



751 References:

- 752 Ahn, Y. and Shanmugam, P.: Derivation and analysis of the fluorescence algorithms to estimate  
753 phytoplankton pigment concentrations in optically, , doi:10.1088/1464-4258/9/4/008, 2007.
- 754 Alamgir, M., Campbell, M. J., Sloan, S., Engert, J., Word, J. and Laurance, W. F.: Emerging challenges  
755 for sustainable development and forest conservation in Sarawak, Borneo, PLoS One, 15(3), 1–20,  
756 doi:10.1371/journal.pone.0229614, 2020.
- 757 Alcântara, E., Bernardo, N., Watanabe, F., Rodrigues, T., Rotta, L., Carmo, A., Shimabukuro, M.,  
758 Gonçalves, S. and Imai, N.: Estimating the CDOM absorption coefficient in tropical inland waters  
759 using OLI/Landsat-8 images, Remote Sens. Lett., 7(7), 661–670,  
760 doi:10.1080/2150704X.2016.1177242, 2016.
- 761 Anthony, K. R. N. and Hoegh-Guldberg, O.: Kinetics of photoacclimation in corals, *Oecologia*, 134(1),  
762 23–31, doi:10.1007/s00442-002-1095-1, 2003.
- 763 Babin, M., Stramski, D., Ferrari, G. M., Claustre, H., Bricaud, A., Obolensky, G. and Hoepffner, N.:  
764 Variations in the light absorption coefficients of phytoplankton, nonalgal particles, and dissolved  
765 organic matter in coastal waters around Europe, , 108, doi:10.1029/2001JC000882, 2003.
- 766 Bailey, S. W., Franz, B. A. and Werdell, P. J.: Estimation of near-infrared water-leaving reflectance for  
767 satellite ocean color data processing, *Opt. Express*, 18(7), 7521, doi:10.1364/oe.18.007521, 2010.
- 768 Balasubramanian, S. V., Pahlevan, N., Smith, B., Binding, C., Schalles, J., Loisel, H., Gurlin, D., Greb, S.,  
769 Alikas, K., Randla, M., Bunkei, M., Moses, W., Nguyễn, H., Lehmann, M. K., O'Donnell, D., Ondrusek,  
770 M., Han, T. H., Fichot, C. G., Moore, T. and Boss, E.: Robust algorithm for estimating total suspended  
771 solids (TSS) in inland and nearshore coastal waters, *Remote Sens. Environ.*, 246(February), 111768,  
772 doi:10.1016/j.rse.2020.111768, 2020.
- 773 Bhardwaj, J., Gupta, K. K. and Gupta, R.: A review of emerging trends on water quality measurement  
774 sensors, *Proc. - Int. Conf. Technol. Sustain. Dev. ICTSD 2015*, (April), 1–6,  
775 doi:10.1109/ICTSD.2015.7095919, 2015.
- 776 Bilotta, G. S. and Brazier, R. E.: Understanding the influence of suspended solids on water quality and  
777 aquatic biota, *Water Res.*, 42(12), 2849–2861, doi:10.1016/j.watres.2008.03.018, 2008.
- 778 Bong, C. H. J. and Richard, J.: Drought and climate change assessment using standardized  
779 precipitation index (Spi) for sarawak river basin, *J. Water Clim. Chang.*, 11(4), 956–965,  
780 doi:10.2166/wcc.2019.036, 2020.
- 781 Cao, F., Tzortziou, M., Hu, C., Mannino, A., Fichot, C. G., Del Vecchio, R., Najjar, R. G. and Novak, M.:  
782 Remote sensing retrievals of colored dissolved organic matter and dissolved organic carbon  
783 dynamics in North American estuaries and their margins, *Remote Sens. Environ.*, 205(November  
784 2017), 151–165, doi:10.1016/j.rse.2017.11.014, 2018.
- 785 Chapman, P. M., Hayward, A. and Faithful, J.: Total Suspended Solids Effects on Freshwater Lake  
786 Biota Other than Fish, *Bull. Environ. Contam. Toxicol.*, 99(4), 423–427, doi:10.1007/s00128-017-  
787 2154-y, 2017.
- 788 Chen, S., Huang, W., Chen, W. and Chen, X.: An enhanced MODIS remote sensing model for  
789 detecting rainfall effects on sediment plume in the coastal waters of Apalachicola Bay, *Mar. Environ.  
790 Res.*, 72(5), 265–272, doi:10.1016/j.marenvres.2011.09.014, 2011.
- 791 Chen, S., Han, L., Chen, X., Li, D., Sun, L. and Li, Y.: Estimating wide range Total Suspended Solids  
792 concentrations from MODIS 250-m imageries: An improved method, *ISPRS J. Photogramm. Remote  
793 Sens.*, 99, 58–69, doi:10.1016/j.isprsjprs.2014.10.006, 2015a.



- 794 Chen, S., Han, L., Chen, X., Li, D., Sun, L. and Li, Y.: Estimating wide range Total Suspended Solids  
795 concentrations from MODIS 250-m imageries: An improved method, *ISPRS J. Photogramm. Remote*  
796 *Sens.*, 99, 58–69, doi:10.1016/j.isprsjprs.2014.10.006, 2015b.
- 797 Chen, Z., Hu, C. and Muller-karger, F.: Monitoring turbidity in Tampa Bay using MODIS / Aqua 250-m  
798 imagery, , 109, 207–220, doi:10.1016/j.rse.2006.12.019, 2007.
- 799 Cherukuru, N., Ford, P. W., Matear, R. J., Oubelkheir, K., Clementson, L. A., Suber, K. and Steven, A.  
800 D. L.: Estimating dissolved organic carbon concentration in turbid coastal waters using optical  
801 remote sensing observations, *Int. J. Appl. Earth Obs. Geoinf.*, 52, 149–154,  
802 doi:10.1016/j.jag.2016.06.010, 2016a.
- 803 Cherukuru, N., Ford, P. W., Matear, R. J., Oubelkheir, K., Clementson, L. A., Suber, K. and Steven, A.  
804 D. L.: Estimating dissolved organic carbon concentration in turbid coastal waters using optical  
805 remote sensing observations, *Int. J. Appl. Earth Obs. Geoinf.*, 52, 149–154,  
806 doi:10.1016/j.jag.2016.06.010, 2016b.
- 807 Cherukuru, N., Martin, P., Sanwlani, N., Mujahid, A. and Müller, M.: A semi-analytical optical remote  
808 sensing model to estimate suspended sediment and dissolved organic carbon in tropical coastal  
809 waters influenced by peatland-draining river discharges off sarawak, borneo, *Remote Sens.*, 13(1), 1–  
810 31, doi:10.3390/rs13010099, 2021.
- 811 Chong, X. Y., Gibbins, C. N., Vericat, D., Batalla, R. J., Teo, F. Y. and Lee, K. S. P.: A framework for  
812 Hydrological characterisation to support Functional Flows (HyFFlow): Application to a tropical river,  
813 *J. Hydrol. Reg. Stud.*, 36(January), doi:10.1016/j.ejrh.2021.100838, 2021.
- 814 CIFOR: Forest Carbon Database, [online] Available from: <https://carbonstock.cifor.org/>, n.d.
- 815 Davies, J., Mathhew, U., Aikanathan, S., Nyon, Y. C. and Chong, G.: A Quick Scan of Peatlands, *Wetl.*  
816 *Int. Malaysia*, 1(March), 1–80, 2010.
- 817 Department of Environment: Malaysia Marine Water Quality Standards and Index, , 16 [online]  
818 Available from: <https://www.doe.gov.my/portalv1/wp-content/uploads/2019/04/BOOKLET-BI.pdf>  
819 (Accessed 12 September 2021), 2019.
- 820 DID: Department of Irrigation & Drainage Sarawak: Introduction to Integrated Coastal Zone  
821 Management, [online] Available from: [https://did.sarawak.gov.my/page-0-123-476-INTEGRATED-](https://did.sarawak.gov.my/page-0-123-476-INTEGRATED-COASTAL-ZONE-MANAGEMENT.html)  
822 [COASTAL-ZONE-MANAGEMENT.html](https://did.sarawak.gov.my/page-0-123-476-INTEGRATED-COASTAL-ZONE-MANAGEMENT.html) (Accessed 21 October 2021a), 2021.
- 823 DID: Department Of Irrigation & Drainage Sarawak, 2021b.
- 824 Dindang, A., Chung, C. N. and Seth, S.: Heavy Rainfall Episodes over Sarawak during January-February  
825 2011 Northeast Monsoon, *JMM Res. Publ.*, (11), 41, 2011.
- 826 Dogliotti, A. I., Ruddick, K. G., Nechad, B., Doxaran, D. and Knaeps, E.: A single algorithm to retrieve  
827 turbidity from remotely-sensed data in all coastal and estuarine waters, *Remote Sens. Environ.*, 156,  
828 157–168, doi:10.1016/j.rse.2014.09.020, 2015.
- 829 Donohue, I. and Garcia Molinos, J.: Impacts of increased sediment loads on the ecology of lakes, *Biol.*  
830 *Rev.*, 84(4), 517–531, doi:10.1111/j.1469-185X.2009.00081.x, 2009.
- 831 Erfteemeijer, P. L. A., Riegl, B., Hoeksema, B. W. and Todd, P. A.: Environmental impacts of dredging  
832 and other sediment disturbances on corals: A review, *Mar. Pollut. Bull.*, 64(9), 1737–1765,  
833 doi:10.1016/j.marpolbul.2012.05.008, 2012.
- 834 Espinoza Villar, R., Martinez, J. M., Le Texier, M., Guyot, J. L., Fraizy, P., Meneses, P. R. and Oliveira,  
835 E. de: A study of sediment transport in the Madeira River, Brazil, using MODIS remote-sensing  
836 images, *J. South Am. Earth Sci.*, 44, 45–54, doi:10.1016/j.jsames.2012.11.006, 2013.



- 837 Fabricius, K. E.: Effects of terrestrial runoff on the ecology of corals and coral reefs: Review and  
838 synthesis, *Mar. Pollut. Bull.*, 50(2), 125–146, doi:10.1016/j.marpolbul.2004.11.028, 2005.
- 839 Fabricius, K. E., Logan, M., Weeks, S. J., Lewis, S. E. and Brodie, J.: Changes in water clarity in  
840 response to river discharges on the Great Barrier Reef continental shelf: 2002-2013, *Estuar. Coast.*  
841 *Shelf Sci.*, 173, A1–A15, doi:10.1016/j.ecss.2016.03.001, 2016.
- 842 Gaveau, D. L. A., Sheil, D., Salim, M. A., Arjasakusuma, S., Ancrenaz, M., Pacheco, P. and Meijaard, E.:  
843 Rapid conversions and avoided deforestation : examining four decades of industrial plantation  
844 expansion in Borneo, *Nat. Publ. Gr.*, (September), 1–13, doi:10.1038/srep32017, 2016.
- 845 Gilmour, J. P., Cooper, T. F., Fabricius, K. E. and Smith, L. D.: Early warning indicators of change in the  
846 condition of corals and coral communities in response to key anthropogenic stressors in the Pilbara,  
847 Western Australia, *Aust. Inst. Mar. Sci. Rep. to Environ. Prot. Authority*. 101pp, 2006.
- 848 Giuliani, G., Chatenoux, B., Piller, T., Moser, F. and Lacroix, P.: Data Cube on Demand (DCoD):  
849 Generating an earth observation Data Cube anywhere in the world, *Int. J. Appl. Earth Obs. Geoinf.*,  
850 87(December 2019), 102035, doi:10.1016/j.jag.2019.102035, 2020.
- 851 Gomes, V. C. F., Carlos, F. M., Queiroz, G. R., Ferreira, K. R. and Santos, R.: Accessing and Processing  
852 Brazilian Earth Observation Data Cubes With the Open Data Cube Platform, *ISPRS Ann. Photogramm.*  
853 *Remote Sens. Spat. Inf. Sci.*, V-4–2021, 153–159, doi:10.5194/isprs-annals-v-4-2021-153-2021, 2021.
- 854 Gomyo, M. and Koichiro, K.: Spatial and temporal variations in rainfall and the ENSO-rainfall  
855 relationship over Sarawak, Malaysian Borneo, *Sci. Online Lett. Atmos.*, 5, 41–44,  
856 doi:10.2151/sola.2009-011, 2009.
- 857 González Vilas, L., Spyrakos, E. and Torres Palenzuela, J. M.: Neural network estimation of  
858 chlorophyll a from MERIS full resolution data for the coastal waters of Galician rias (NW Spain),  
859 *Remote Sens. Environ.*, 115(2), 524–535, doi:10.1016/j.rse.2010.09.021, 2011.
- 860 Ha, N. T. T., Thao, N. T. P., Koike, K. and Nhuan, M. T.: Selecting the best band ratio to estimate  
861 chlorophyll-a concentration in a tropical freshwater lake using sentinel 2A images from a case study  
862 of Lake Ba Be (Northern Vietnam), *ISPRS Int. J. Geo-Information*, 6(9), doi:10.3390/ijgi6090290,  
863 2017.
- 864 Henley, W. F., Patterson, M. A., Neves, R. J. and Dennis Lemly, A.: Effects of Sedimentation and  
865 Turbidity on Lotic Food Webs: A Concise Review for Natural Resource Managers, *Rev. Fish. Sci.*, 8(2),  
866 125–139, doi:10.1080/10641260091129198, 2000.
- 867 Hodgson, G.: Tetracycline reduces sedimentation damage to corals, *Mar. Biol.*, 104(3), 493–496,  
868 1990.
- 869 Hon, J. and Shibata, S.: A Review on Land Use in the Malaysian State of Sarawak, Borneo and  
870 Recommendations for Wildlife Conservation Inside Production Forest Environment, *Borneo J.*  
871 *Resour. Sci. Technol.*, 3(2), 22–35, doi:10.33736/bjrst.244.2013, 2013.
- 872 Horsburgh, J. S., Spackman, A., Stevens, D. K., Tarboton, D. G. and Mesner, N. O.: Environmental  
873 Modelling & Software A sensor network for high frequency estimation of water quality constituent  
874 fluxes using surrogates, , 25, 1031–1044, doi:10.1016/j.envsoft.2009.10.012, 2010.
- 875 Howarth, R. W.: Coastal nitrogen pollution: A review of sources and trends globally and regionally,  
876 *Harmful Algae*, 8(1), 14–20, doi:10.1016/j.hal.2008.08.015, 2008.
- 877 Hu, C., Lee, Z. and Franz, B.: Chlorophyll a algorithms for oligotrophic oceans: A novel approach  
878 based on three-band reflectance difference, *J. Geophys. Res. Ocean.*, 117(1), 1–25,  
879 doi:10.1029/2011JC007395, 2012.



- 880 Jiang, D., Matsushita, B., Pahlevan, N., Gurlin, D., Lehmann, M. K., Fichot, C. G., Schalles, J., Loisel, H.,  
881 Binding, C., Zhang, Y., Alikas, K., Kangro, K., Uusõue, M., Ondrusek, M., Greb, S., Moses, W. J.,  
882 Lohrenz, S. and O'Donnell, D.: Remotely estimating total suspended solids concentration in clear to  
883 extremely turbid waters using a novel semi-analytical method, *Remote Sens. Environ.*, 258,  
884 doi:10.1016/j.rse.2021.112386, 2021.
- 885 Jiang, H. and Liu, Y.: Monitoring of TSS concentration in Poyang Lake based on MODIS data, *Yangtze*  
886 *River*, 42(17), 87–90, 2011.
- 887 Kemp, P., Sear, D., Collins, A., Naden, P. and Jones, I.: The impacts of fine sediment on riverine fish,  
888 *Hydrol. Process.*, 25(11), 1800–1821, doi:10.1002/hyp.7940, 2011.
- 889 Killough, B.: The Impact of Analysis Ready Data in the Africa Regional Data Cube, *Int. Geosci. Remote*  
890 *Sens. Symp.*, (July 2019), 5646–5649, doi:10.1109/IGARSS.2019.8898321, 2019.
- 891 Kim, H. C., Son, S., Kim, Y. H., Khim, J. S., Nam, J., Chang, W. K., Lee, J. H., Lee, C. H. and Ryu, J.:  
892 Remote sensing and water quality indicators in the Korean West coast: Spatio-temporal structures of  
893 MODIS-derived chlorophyll-a and total suspended solids, *Mar. Pollut. Bull.*, 121(1–2), 425–434,  
894 doi:10.1016/j.marpolbul.2017.05.026, 2017.
- 895 Krause, C., Dunn, B., Bishop-Taylor, R., Adams, C., Burton, C., Alger, M., Chua, S., Phillips, C., Newey,  
896 V., Kouzoubov, K., Leith, A., Ayers, D., Hicks, A. and DEA Notebooks contributors 2021: Digital Earth  
897 Australia notebooks and tools repository, , doi:https://doi.org/10.26186/145234, 2021.
- 898 Langer, O. E.: Effects of sedimentation on salmonid stream life, *Environmental Protection Service.*,  
899 1980.
- 900 Lavigne, H., Van der Zande, D., Ruddick, K., Cardoso Dos Santos, J. F., Gohin, F., Brotas, V. and  
901 Kratzer, S.: Quality-control tests for OC4, OC5 and NIR-red satellite chlorophyll-a algorithms applied  
902 to coastal waters, *Remote Sens. Environ.*, 255, 112237, doi:10.1016/j.rse.2020.112237, 2021.
- 903 Lee, K. H., Noh, J. and Khim, J. S.: The Blue Economy and the United Nations' sustainable  
904 development goals: Challenges and opportunities, *Environ. Int.*, 137(October 2019), 105528,  
905 doi:10.1016/j.envint.2020.105528, 2020a.
- 906 Lee, W. C., Viswanathan, K. K., Kamri, T. and King, S.: Status of Sarawak Fisheries: Challenges and  
907 Way Forward, *Int. J. Serv. Manag. Sustain.*, 5(2), 187–200, doi:10.24191/ijms.v5i2.11719, 2020b.
- 908 Lemley, D. A., Adams, J. B., Bornman, T. G., Campbell, E. E. and Deyzel, S. H. P.: Land-derived  
909 inorganic nutrient loading to coastal waters and potential implications for nearshore plankton  
910 dynamics, *Cont. Shelf Res.*, 174(August 2018), 1–11, doi:10.1016/j.csr.2019.01.003, 2019.
- 911 Lewis, A., Oliver, S., Lymburner, L., Evans, B., Wyborn, L., Mueller, N., Raevksi, G., Hooke, J.,  
912 Woodcock, R., Sixsmith, J., Wu, W., Tan, P., Li, F., Killough, B., Minchin, S., Roberts, D., Ayers, D.,  
913 Bala, B., Dwyer, J., Dekker, A., Dhu, T., Hicks, A., Ip, A., Purss, M., Richards, C., Sagar, S., Trenham, C.,  
914 Wang, P. and Wang, L. W.: The Australian Geoscience Data Cube — Foundations and lessons  
915 learned, *Remote Sens. Environ.*, 202, 276–292, doi:10.1016/j.rse.2017.03.015, 2017.
- 916 Limchih, F., Jilnm, M., Hb, H., Ilcach, H. N. M., Mnl, F., Fi, F. and Nb, F.: Study of Coastal Areas in Miri,  
917 in *World Engineering Congress 2010*, pp. 56–65., 2010.
- 918 Ling, T. Y., Soo, C. L., Sivalingam, J. R., Nyanti, L., Sim, S. F. and Grinang, J.: Assessment of the Water  
919 and Sediment Quality of Tropical Forest Streams in Upper Reaches of the Baleh River, Sarawak,  
920 Malaysia, Subjected to Logging Activities, *J. Chem.*, 2016, doi:10.1155/2016/8503931, 2016.
- 921 Liu, B., D'Sa, E. J. and Joshi, I.: Multi-decadal trends and influences on dissolved organic carbon  
922 distribution in the Barataria Basin, Louisiana from in-situ and Landsat/MODIS observations, *Remote*



- 923 Sens. Environ., 228(May), 183–202, doi:10.1016/j.rse.2019.04.023, 2019.
- 924 Loisel, H., Mangin, A., Vantrepotte, V., Dessailly, D., Ngoc Dinh, D., Garnesson, P., Ouillon, S.,  
925 Lefebvre, J. P., Mériaux, X. and Minh Phan, T.: Variability of suspended particulate matter  
926 concentration in coastal waters under the Mekong's influence from ocean color (MERIS) remote  
927 sensing over the last decade, Remote Sens. Environ., 150, 218–230, doi:10.1016/j.rse.2014.05.006,  
928 2014.
- 929 Long, S. M.: Sarawak Coastal Biodiversity : A Current Status, Kuroshio Sci., 8(1), 71–84 [online]  
930 Available from: <https://www.researchgate.net/publication/265793245>, 2014.
- 931 Lu, Y., Yuan, J., Lu, X., Su, C., Zhang, Y., Wang, C., Cao, X., Li, Q., Su, J., Ittekkot, V., Garbutt, R. A.,  
932 Bush, S., Fletcher, S., Wagey, T., Kachur, A. and Sweijd, N.: Major threats of pollution and climate  
933 change to global coastal ecosystems and enhanced management for sustainability, Environ. Pollut.,  
934 239, 670–680, doi:10.1016/j.envpol.2018.04.016, 2018.
- 935 Macklin, M. G., Jones, A. F. and Lewin, J.: River response to rapid Holocene environmental change:  
936 evidence and explanation in British catchments, Quat. Sci. Rev., 29(13–14), 1555–1576,  
937 doi:10.1016/j.quascirev.2009.06.010, 2010.
- 938 Mao, Z., Chen, J., Pan, D., Tao, B. and Zhu, Q.: A regional remote sensing algorithm for total  
939 suspended matter in the East China Sea, Remote Sens. Environ., 124, 819–831,  
940 doi:10.1016/j.rse.2012.06.014, 2012.
- 941 Martin, P., Cherukuru, N., Tan, A. S. Y., Sanwlan, N., Mujahid, A. and Müller, M.: Distribution and  
942 cycling of terrigenous dissolved organic carbon in peatland-draining rivers and coastal waters of  
943 Sarawak, Borneo, Biogeosciences, 15(22), 6847–6865, doi:10.5194/bg-15-6847-2018, 2018.
- 944 Mengen, D., Ottinger, M., Leinenkugel, P. and Ribbe, L.: Modeling river discharge using automated  
945 river width measurements derived from sentinel-1 time series, Remote Sens., 12(19), 1–24,  
946 doi:10.3390/rs12193236, 2020.
- 947 Mohammad Razi, M. A., Mokhtar, A., Mahamud, M., Rahmat, S. N. and Al-Gheethi, A.: Monitoring of  
948 river and marine water quality at Sarawak baseline, Environ. Forensics, 22(1–2), 219–240,  
949 doi:10.1080/15275922.2020.1836076, 2021.
- 950 Morel, A. and Bélanger, S.: Improved detection of turbid waters from ocean color sensors  
951 information, Remote Sens. Environ., 102(3–4), 237–249, doi:10.1016/j.rse.2006.01.022, 2006.
- 952 Morel, A. and Gentili, B.: A simple band ratio technique to quantify the colored dissolved and detrital  
953 organic material from ocean color remotely sensed data, Remote Sens. Environ., 113(5), 998–1011,  
954 doi:10.1016/j.rse.2009.01.008, 2009.
- 955 Mueller, J., Mueller, J., Pietras, C., Hooker, S., Clark, D., Frouin, A., Mitchell, B., Bidigare, R., Trees, C.  
956 and Werdell, J.: Ocean Optics Protocols For Satellite Ocean Color Sensor Validation, Revision 3,  
957 volumes 1 and 2., 2002.
- 958 Müller-dum, D., Warneke, T., Rixen, T., Müller, M., Baum, A., Christodoulou, A., Oakes, J., Eyre, B. D.  
959 and Notholt, J.: Impact of peatlands on carbon dioxide ( CO<sub>2</sub> ) emissions from the Rajang River and  
960 Estuary , Malaysia , , 17–32, 2019.
- 961 Müller, D., Warneke, T., Rixen, T., Müller, M., Mujahid, A., Bange, H. W. and Notholt, J.: Fate of  
962 terrestrial organic carbon and associated CO<sub>2</sub> and CO emissions from two Southeast Asian estuaries,  
963 Biogeosciences, 13(3), 691–705, doi:10.5194/bg-13-691-2016, 2016.
- 964 NASA Official: Ocean Level-2 Data Format Specification, [online] Available from:  
965 <https://oceancolor.gsfc.nasa.gov/docs/format/l2nc/>, n.d.



- 966 Nazirova, K., Alferyeva, Y., Lavrova, O., Shur, Y., Soloviev, D., Bocharova, T. and Stochkov, A.:  
967 Comparison of in situ and remote-sensing methods to determine turbidity and concentration of  
968 suspended matter in the estuary zone of the mzymta river, black sea, *Remote Sens.*, 13(1), 1–29,  
969 doi:10.3390/rs13010143, 2021.
- 970 Neil, C., Spyarakos, E., Hunter, P. D. and Tyler, A. N.: A global approach for chlorophyll-a retrieval  
971 across optically complex inland waters based on optical water types, *Remote Sens. Environ.*,  
972 229(May), 159–178, doi:10.1016/j.rse.2019.04.027, 2019.
- 973 Omorinoye, O. A., Assim, Z. Bin and Jusoh, I. Bin: Geomorphological and Sedimentological Features  
974 of River Sadong, Sarawak, Malaysia, *Indones. J. Geosci.*, 8(1), 119–130, doi:10.17014/ijog.8.1.119-  
975 130, 2021.
- 976 Ondrusek, M., Stengel, E., Kinkade, C. S., Vogel, R. L., Keegstra, P., Hunter, C. and Kim, C.: The  
977 development of a new optical total suspended matter algorithm for the Chesapeake Bay, *Remote*  
978 *Sens. Environ.*, 119, 243–254, doi:10.1016/j.rse.2011.12.018, 2012.
- 979 Open Data Cube: Open Data Cube, [online] Available from:  
980 <https://opendatacube.readthedocs.io/en/latest/user/intro.html> (Accessed 25 October 2021), 2021.
- 981 Park, G. S.: The role and distribution of total suspended solids in the macrotidal coastal waters of  
982 Korea, *Environ. Monit. Assess.*, 135(1–3), 153–162, doi:10.1007/s10661-007-9640-3, 2007.
- 983 Petus, C., Marieu, V., Novoa, S., Chust, G., Bruneau, N. and Froidefond, J. M.: Monitoring spatio-  
984 temporal variability of the Adour River turbid plume (Bay of Biscay, France) with MODIS 250-m  
985 imagery, *Cont. Shelf Res.*, 74, 35–49, doi:10.1016/j.csr.2013.11.011, 2014.
- 986 Praveena, S. M., Siraj, S. S. and Aris, A. Z.: Coral reefs studies and threats in Malaysia: A mini review,  
987 *Rev. Environ. Sci. Biotechnol.*, 11(1), 27–39, doi:10.1007/s11157-011-9261-8, 2012.
- 988 Ramaswamy, V., Rao, P. S., Rao, K. H., Thwin, S., Rao, N. S. and Raiker, V.: Tidal influence on  
989 suspended sediment distribution and dispersal in the northern Andaman Sea and Gulf of Martaban,  
990 *Mar. Geol.*, 208(1), 33–42, doi:10.1016/j.margeo.2004.04.019, 2004.
- 991 Refaeilzadeh, P., Tang, L., Liu, H., Angeles, L. and Scientist, C. D.: Encyclopedia of Database Systems,  
992 *Encycl. Database Syst.*, doi:10.1007/978-1-4899-7993-3, 2020.
- 993 Risk, M. J. and Edinger, E.: Impacts of sediment on coral reefs, *Encycl. Mod. coral reefs*. Springer,  
994 Netherlands, 575–586, 2011.
- 995 Rogers, C. S.: The effect of shading on coral reef structure and function, *J. Exp. Mar. Bio. Ecol.*, 41(3),  
996 269–288, doi:10.1016/0022-0981(79)90136-9, 1979.
- 997 Sa’adi, Z., Shahid, S., Chung, E. S. and Ismail, T. bin: Projection of spatial and temporal changes of  
998 rainfall in Sarawak of Borneo Island using statistical downscaling of CMIP5 models, *Atmos. Res.*,  
999 197(November 2016), 446–460, doi:10.1016/j.atmosres.2017.08.002, 2017.
- 1000 Sandifer, P. A., Keener, P., Scott, G. I. and Porter, D. E.: Oceans and Human Health and the New Blue  
1001 Economy, Elsevier Inc., 2021.
- 1002 Seegers, B. N., Stumpf, R. P., Schaeffer, B. A., Loftin, K. A. and Werdell, P. J.: Performance metrics for  
1003 the assessment of satellite data products: an ocean color case study, *Opt. Express*, 26(6), 7404,  
1004 doi:10.1364/oe.26.007404, 2018.
- 1005 Shaw, E. Al and Richardson, J. S.: Direct and indirect effects of sediment pulse duration on stream  
1006 invertebrate assemblages and rainbow trout (*Oncorhynchus mykiss*) growth and survival, *Can. J.*  
1007 *Fish. Aquat. Sci.*, 58(11), 2213–2221, doi:10.1139/f01-160, 2001.



- 1008 Sim, C., Cherukuru, N., Mujahid, A., Martin, P., Sanwani, N., Warneke, T., Rixen, T., Notholt, J. and  
1009 Müller, M.: A new remote sensing method to estimate river to ocean DOC flux in peatland  
1010 dominated Sarawak coastal regions, Borneo, *Remote Sens.*, 12(20), 1–13, doi:10.3390/rs12203380,  
1011 2020.
- 1012 Siswanto, E., Tang, J. and Yamaguchi, H.: Empirical ocean-color algorithms to retrieve chlorophyll- a ,  
1013 total suspended matter , and colored dissolved organic matter absorption coefficient in the Yellow  
1014 and East China Seas , 627–650, doi:10.1007/s10872-011-0062-z, 2011.
- 1015 Slonecker, E. T., Jones, D. K. and Pellerin, B. A.: The new Landsat 8 potential for remote sensing of  
1016 colored dissolved organic matter (CDOM), *Mar. Pollut. Bull.*, 107(2), 518–527,  
1017 doi:10.1016/j.marpolbul.2016.02.076, 2016.
- 1018 Song, C., Wang, G., Sun, X., Chang, R. and Mao, T.: Control factors and scale analysis of annual river  
1019 water, sediments and carbon transport in China, *Sci. Rep.*, 6(May), 1–14, doi:10.1038/srep25963,  
1020 2016.
- 1021 Song, Z., Shi, W., Zhang, J., Hu, H., Zhang, F. and Xu, X.: Transport mechanism of suspended  
1022 sediments and migration trends of sediments in the central hangzhou bay, *Water (Switzerland)*,  
1023 12(8), doi:10.3390/W12082189, 2020.
- 1024 Soo, C. L., Chen, C. A. and Mohd-Long, S.: Assessment of Near-Bottom Water Quality of  
1025 Southwestern Coast of Sarawak, Borneo, Malaysia: A Multivariate Statistical Approach, *J. Chem.*,  
1026 2017, doi:10.1155/2017/1590329, 2017.
- 1027 Soum, S., Ngor, P. B., Dilts, T. E., Lohani, S., Kelson, S., Null, S. E., Tromboni, F., Hogan, Z. S., Chan, B.  
1028 and Chandra, S.: Spatial and long-term temporal changes in water quality dynamics of the tonle sap  
1029 ecosystem, *Water (Switzerland)*, 13(15), doi:10.3390/w13152059, 2021.
- 1030 Staub, J. R., Among, H. L. and Gastaldo, R. A.: Seasonal sediment transport and deposition in the  
1031 Rajang River delta, Sarawak, East Malaysia, *Sediment. Geol.*, 133(3–4), 249–264, doi:10.1016/S0037-  
1032 0738(00)00042-7, 2000.
- 1033 Sun, C.: Riverine influence on ocean color in the equatorial South China Sea, *Cont. Shelf Res.*,  
1034 143(December 2015), 151–158, doi:10.1016/j.csr.2016.10.008, 2017a.
- 1035 Sun, C.: Riverine influence on ocean color in the equatorial South China Sea, *Cont. Shelf Res.*,  
1036 143(October 2016), 151–158, doi:10.1016/j.csr.2016.10.008, 2017b.
- 1037 Sutherland, A. B. and Meyer, J. L.: Effects of increased suspended sediment on growth rate and gill  
1038 condition of two southern Appalachian minnows, *Environ. Biol. Fishes*, 80(4), 389–403,  
1039 doi:10.1007/s10641-006-9139-8, 2007.
- 1040 Swain, R. and Sahoo, B.: Mapping of heavy metal pollution in river water at daily time-scale using  
1041 spatio-temporal fusion of MODIS-aqua and Landsat satellite imageries, *J. Environ. Manage.*, 192, 1–  
1042 14, doi:10.1016/j.jenvman.2017.01.034, 2017.
- 1043 Tangang, F. T., Juneng, L., Salimun, E., Sei, K. M., Le, L. J. and Muhamad, H.: Climate change and  
1044 variability over Malaysia: Gaps in science and research information, *Sains Malaysiana*, 41(11), 1355–  
1045 1366, 2012.
- 1046 Tawan, A. S., Ling, T. Y., Nyanti, L., Sim, S. F., Grinang, J., Soo, C. L., Lee, K. S. P. and Ganyai, T.:  
1047 Assessment of water quality and pollutant loading of the Rajang River and its tributaries at Pelagus  
1048 area subjected to seasonal variation and river regulation, *Environ. Dev. Sustain.*, 22(5), 4101–4124,  
1049 doi:10.1007/s10668-019-00374-9, 2020.
- 1050 Telesnicki, G. J. and Goldberg, W. M.: CORAL REEF PAPER EFFECTS OF TURBIDITY ON THE



- 1051 PHOTOSYNTHESIS AND RESPIRATION OF TWO SOUTH FLORIDA REEF CORAL SPECIES portant factors  
1052 in the regulation of coral cover , diversity , and abundance ( Ed- ships between suspended sediment  
1053 concentrations or parti , , 57(2), 527–539, 1995.
- 1054 Tilburg, C. E., Jordan, L. M., Carlson, A. E., Zeeman, S. I. and Yund, P. O.: The effects of precipitation,  
1055 river discharge, land use and coastal circulation on water quality in coastal Maine, *R. Soc. Open Sci.*,  
1056 2(7), doi:10.1098/rsos.140429, 2015.
- 1057 Tromboni, F., Dilts, T. E., Null, S. E., Lohani, S., Ngor, P. B., Soum, S., Hogan, Z. and Chandra, S.:  
1058 Changing land use and population density are degrading water quality in the lower mekong basin,  
1059 *Water (Switzerland)*, 13(14), 1–16, doi:10.3390/w13141948, 2021.
- 1060 United Nations: The Ocean Conference, in *The Ocean Conference*, vol. 53, p. 130, New York., 2017.
- 1061 Valerio, A. de M., Kampel, M., Vantrepotte, V., Ward, N. D., Sawakuchi, H. O., Less, D. F. D. S., Neu,  
1062 V., Cunha, A. and Richey, J.: Using CDOM optical properties for estimating DOC concentrations and  
1063 pCO<sub>2</sub> in the Lower Amazon River , *Opt. Express*, 26(14), A657, doi:10.1364/oe.26.00a657, 2018.
- 1064 Verschelling, E., van der Deijl, E., van der Perk, M., Sloff, K. and Middelkoop, H.: Effects of discharge,  
1065 wind, and tide on sedimentation in a recently restored tidal freshwater wetland, *Hydrol. Process.*,  
1066 31(16), 2827–2841, doi:10.1002/hyp.11217, 2017.
- 1067 Vijith, H., Hurmain, A. and Dodge-Wan, D.: Impacts of land use changes and land cover alteration on  
1068 soil erosion rates and vulnerability of tropical mountain ranges in Borneo, *Remote Sens. Appl. Soc.*  
1069 *Environ.*, 12(September), 57–69, doi:10.1016/j.rsase.2018.09.003, 2018.
- 1070 Wang, C., Chen, S., Li, D., Wang, D., Liu, W. and Yang, J.: A Landsat-based model for retrieving total  
1071 suspended solids concentration of estuaries and coasts in China, *Geosci. Model Dev.*, 10(12), 4347–  
1072 4365, doi:10.5194/gmd-10-4347-2017, 2017.
- 1073 Wang, J., Tong, Y., Feng, L., Zhao, D., Zheng, C. and Tang, J.: Satellite-Observed Decreases in Water  
1074 Turbidity in the Pearl River Estuary: Potential Linkage With Sea-Level Rise, *J. Geophys. Res. Ocean.*,  
1075 126(4), 1–17, doi:10.1029/2020JC016842, 2021.
- 1076 Weber, M., Lott, C. and Fabricius, K. E.: Sedimentation stress in a scleractinian coral exposed to  
1077 terrestrial and marine sediments with contrasting physical, organic and geochemical properties, *J.*  
1078 *Exp. Mar. Bio. Ecol.*, 336(1), 18–32, doi:10.1016/j.jembe.2006.04.007, 2006.
- 1079 Werdell, P. J., McKinna, L. I. W., Boss, E., Ackleson, S. G., Craig, S. E., Gregg, W. W., Lee, Z.,  
1080 Maritorena, S., Roesler, C. S., Rousseaux, C. S., Stramski, D., Sullivan, J. M., Twardowski, M. S.,  
1081 Tzortziou, M. and Zhang, X.: An overview of approaches and challenges for retrieving marine  
1082 inherent optical properties from ocean color remote sensing, *Prog. Oceanogr.*, 160, 186–212,  
1083 doi:10.1016/j.pocean.2018.01.001, 2018.
- 1084 Whitmore, T. C.: *Tropical rain forests of the Par East*, Oxford. Clarendon Press., 1984.
- 1085 Wilber, D. H. and Clarke, D. G.: Biological Effects of Suspended Sediments: A Review of Suspended  
1086 Sediment Impacts on Fish and Shellfish with Relation to Dredging Activities in Estuaries, *North Am. J.*  
1087 *Fish. Manag.*, 21(4), 855–875, doi:10.1577/1548-8675(2001)021<0855:beossa>2.0.co;2, 2001.
- 1088 World Bank and United Nations Department of Economic and Social Affairs (UNDESA): *The Potential*  
1089 *of the Blue Economy: Increasing Long-term Benefits of the Sustainable Use of Marine Resources for*  
1090 *Small Island Developing States and Coastal Least Developed Countries*, World Bank, Washington DC.,  
1091 2017.
- 1092 Wu, C. S., Yang, S. L. and Lei, Y. ping: Quantifying the anthropogenic and climatic impacts on water  
1093 discharge and sediment load in the Pearl River (Zhujiang), China (1954–2009), *J. Hydrol.*, 452–453,



1094 190–204, doi:10.1016/j.jhydrol.2012.05.064, 2012.

1095 Yang, S. L., Zhao, Q. Y. and Belkin, I. M.: Temporal variation in the sediment load of the Yangtze river  
1096 and the influences of human activities, *J. Hydrol.*, 263(1–4), 56–71, doi:10.1016/S0022-  
1097 1694(02)00028-8, 2002.

1098 Zhan, W., Wu, J., Wei, X., Tang, S. and Zhan, H.: Spatio-temporal variation of the suspended  
1099 sediment concentration in the Pearl River Estuary observed by MODIS during 2003–2015, *Cont. Shelf*  
1100 *Res.*, 172(May 2018), 22–32, doi:10.1016/j.csr.2018.11.007, 2019.

1101 Zhang, L. J., Wang, L., Cai, W. J., Liu, D. M. and Yu, Z. G.: Impact of human activities on organic carbon  
1102 transport in the Yellow River, *Biogeosciences*, 10(4), 2513–2524, doi:10.5194/bg-10-2513-2013,  
1103 2013.

1104 Zhang, M., Tang, J., Dong, Q., Song, Q. T. and Ding, J.: Retrieval of total suspended matter  
1105 concentration in the Yellow and East China Seas from MODIS imagery, *Remote Sens. Environ.*,  
1106 114(2), 392–403, doi:10.1016/j.rse.2009.09.016, 2010a.

1107 Zhang, Y., Lin, S., Liu, J., Qian, X. and Ge, Y.: Time-series MODIS image-based retrieval and  
1108 distribution analysis of total suspended matter concentrations in Lake Taihu (China), *Int. J. Environ.*  
1109 *Res. Public Health*, 7(9), 3545–3560, doi:10.3390/ijerph7093545, 2010b.

1110 Zhou, Y., Xuan, J. and Huang, D.: Tidal variation of total suspended solids over the Yangtze Bank  
1111 based on the geostationary ocean color imager, *Sci. China Earth Sci.*, 63(9), 1381–1389,  
1112 doi:10.1007/s11430-019-9618-7, 2020.

1113

1114

1115

1116

1117

1118

1119

1120

1121

1122

1123

1124

1125

1126

1127

1128

1129